

# The Role of Nuclear Thermal-Hydraulics in the Licensing of Atucha-II: the LBLOCA

Oscar Mazzantini<sup>1</sup>, Giorgio Galassi<sup>2</sup> and Francesco D'Auria<sup>2,\*</sup>

<sup>1</sup> NA-SA; mazzantini@na-sa.com.ar

<sup>2</sup> University of Pisa: g.galass@ing.unipi.it

\* Corresponding author. University of Pisa: f.dauria@ing.unipi.it; Tel.: (+39-050-2210-359)

**Abstract:** The paper deals with the safety evaluation and the embedded licensing process of the Atucha-II 800 Mwe Pressurized Heavy Water Reactor (PHWR) in Argentina. Atucha-II was designed by Kraftwerk Union (KWU) during the 60's, the related construction was started/stopped in the 90's and restarted on 2006, and was connected to the electrical grid in 2014. Because of market policies, the KWU designer could not be directly involved in the licensing process during the first decade of the 2000 millennium: a licensing suited safety evaluation was performed by the Nucleoeléctrica Argentina (NA-SA), utility owner of the Atucha-II, with support of external experts group. A designer-independent assessment was performed having access to the installed systems and components other than the relevant design documents. Large core size (related to Pressurized Water Reactor – PWR – producing the same thermal power), presence in the core of natural uranium and heavy water fluids, i.e. the coolant and the moderator driven by two circulation loops with different average temperatures, characterize the system design. In those conditions, during the early phase of a depressurization transient, the 'hot' coolant vaporizes and the colder moderator remains in the liquid phase: a positive void coefficient is created. The relevance of the Large Break Loss of Coolant Accident (LBLOCA) in safety assessment is discussed with emphasis given to the system design features, the approach pursued in the analysis and the key results. Break opening time and time of occurrence of the safety boron injection affect, during the early period of the transient, the propagation of (negative) pressure wave, the fluid flashing, the heat transfer and the neutron flux: a fission power excursion is expected to occur. The analysis of a complex three-dimensional situation, considering the unavoidable uncertainties associated with the computation, demonstrates that safety limits are preserved.

**Keywords:** Atucha-II; PHWR; Channel type reactor; Positive void coefficient; LBLOCA; BEPU approach

## 1. Introduction

Nuclear Reactor Safety (NRS) may be defined as the connection between the protection of the environment and the humans against the ionizing radiations massively produced and stored in the core of Nuclear Power Plants, [IAEA, 2000](#).

Accident Analysis (AA) constitutes a key part of NRS: triggering and system availability for transients events are assumed with a given probability within the Design Basis Accident (DBA) boundary and response of the concerned reactor is evaluated with the purpose of demonstrating the available safety margins, [IAEA, 2002](#). However, deterministic analyses have to cover pre-determined events independent of probabilities.

The Loss of Coolant Accident (LOCA) is an element of the DBA set of accidents, [OECD/NEA/CSNI, 1989](#); in the case of Pressurized Water Reactors (PWR), the LOCA term implies a group of accidents primarily characterized by different break area and location. In most situations,

45 the Large Break LOCA (LBLOCA), which is strictly connected with the reactor design (chapter 2), is  
46 originated by the Double Ended Guillotine Break (DEGB) in one Cold Leg (CL) close to the Reactor  
47 Pressure Vessel (RPV).

48 Licensing constitutes the legal part of NRS or the connection between results from safety  
49 analyses and threshold limits set by regulators, e.g. [USNRC, 2005](#): any licensing analysis includes a  
50 safety evaluation performed according to hypotheses and procedures consistent with the regulatory  
51 process.

52 A wide literature exists for LBLOCA in PWR see e.g. [D'Auria & Galassi, 2017](#), and [Ylonen A.,  
53 2008](#). A cross-link between design features of reactors, accident scenarios, phenomena and  
54 parameters relevant to phenomena, is established; LOCA related topics can be distinguished into six  
55 broad categories which are briefly discussed hereafter including main findings: 1) the dynamic  
56 effects; 2) the core cooling and the Peak Cladding Temperature (PCT); 3) the nuclear fuel behavior; 4)  
57 the containment performance; 5) the long term cooling; 6) the licensing aspects and the application  
58 of the Best Estimate Plus Uncertainty (BEPU) approach.

59 The dynamic effects are originated by the break opening and consequent connection between  
60 space-regions at different pressures, or primary system and containment at 15 and 0.1 MPa,  
61 respectively. The fluid depressurization wave and the stored energy in the metal structure of the  
62 piping generate loads upon primary system internals (primarily inside RPV), e.g. [Vigni et al., 1978](#),  
63 and [D'Auria & Vigni, 1989](#), and containment (see below). The amplitude of pressure wave generated  
64 at the break depends upon the break opening time (as discussed with more detail in section 3.1);  
65 consequent load effects arise in about 1 s since the break opening occurrence owing to the sonic  
66 speed propagation of the wave.

67 The core cooling has been at the center of attention of nuclear thermal-hydraulics since the 50's  
68 of the XX century. Related to LBLOCA well known terms are summarized as blowdown, refill,  
69 reflood, Departure from Nuclear Boiling (DNB), PCT, Two-Phase Critical Flow (TPCF) and  
70 design/actuation of Emergency Core Cooling Systems (ECCS), see e.g. [Aksan et al., 2018](#), [Petruzzi &  
71 D'Auria, 2005](#), and [OECD/NEA/CSNI, 1989](#).

72 The fuel behavior needs specific consideration during LOCA because of a three-fold solicitation  
73 of the clad after the mentioned pressure wave load: (a) high temperature following the DNB  
74 occurrence with reduced mechanical strength, (b) large pressure differential when inside fission gas  
75 pressure remains nearly constant and external system pressure decreases following the system  
76 depressurization, and (c) fast chemical reaction with water and consequent oxidization and  
77 embrittlement. Clad ballooning and burst, other than hydrogen production may result originating  
78 concerns in relation to core cooling and release of fission products into the coolant, [OECD/NEA,  
79 2009](#). Additional fuel weaknesses have been characterized during the last decade leading to  
80 concerns, e.g. [D'Auria et al., 2018](#), (see also [D'Auria et al., 2019](#)) in relation to capability of the fuel to  
81 satisfy the criteria set for the ECCS design, [USAEC, 1971](#), and [USNRC, 2018](#).

82 The containment constitutes the ultimate heavy barrier to the release of fission products  
83 installed to protect humans and environment in case of failures of other safety barriers. Pressure and  
84 temperature loads following LOCA constitute design targets for the containment,  
85 [OECD/NEA/CSNI, 1999](#). Dynamic loads acting on the containment can be classified as jet thrust and  
86 primary system restraints, e.g. [Vigni & D'Auria, 1979](#), pipe whip, e.g. [Reid et al., 2011](#), and missile,  
87 [Ranjan et al., 2014](#).

88 The demonstration of the long term cooling capability is part of early requirements for water  
89 cooled nuclear reactors, [USAEC, 1971](#). Recent findings and consideration of the licensing rule can be  
90 found in [Ullah Amin et al., 2017](#). The presence of LOCA generated debris on the pool constitutes a  
91 concern in nuclear reactor safety, e.g. [Park et al., 2011](#),

92 The licensing aspects and the BEPU imply the application of a computer code, e.g. Relap,  
93 [RELAP5/MOD3, 1998](#), and of a regulation, e.g. [USNRC, 2005](#), (already cited) see also [USNRC, 1978](#),  
94 and [USNRC, 2007](#), to the analysis of any accident scenario including LBLOCA. Then, the application  
95 of a computer code implies the development and the qualification of the code, e.g. [D'Auria &  
96 Galassi, 1998](#), as well as of the nodalization, e.g. [Bonuccelli et al., 1993](#), and the code-user or analyst,  
97 e.g. [Ashley et al., 1998](#). Addressing the scaling issue, e.g. [OECD/NEA/CSNI, 2017](#), coupling of codes,

98 e.g. OECD/NEA, 2004, see also Bousbia-Salah et al., 2004, and uncertainty evaluation, e.g. IAEA,  
99 2008, constitute essential elements of the BEPU approach which also needs a formal procedure, e.g.  
100 D’Auria et al., 2012, see also Galetti & D’Auria, 2004, and Kang, 2016.

101 The peculiarities associated with the use of heavy water as moderator, i.e. Pressurized Heavy  
102 Water Reactors (PHWR) strongly affect the LOCA scenario. Two main types of reactors can be  
103 classified as PHWR: the Canadian Deuterium-Uranium (CANDU) and the Atucha reactors (I and II  
104 units). Heavy water is used in order to allow natural uranium as fuel; cylindrical channel boxes  
105 separate coolant and moderator: in the case of CANDU, horizontal pressurized fuel channel separate  
106 the coolant from the nearly-at-atmospheric-pressure heavy water moderator; in the case of Atucha,  
107 vertical fuel channels are installed inside the RPV which keeps nearly at the same pressure the  
108 moderator and the coolant. In both cases average moderator temperature is lower than coolant  
109 temperature (much lower in the case of CANDU). LOCA accident generates a fission power peak in  
110 both PHWR types, e.g. see Kastanya et al., 2013, in the case of CANDU and Pecchia et al., 2015, and  
111 Mazzantini et al., 2018, in the case of the Atucha-II PHWR: coolant vaporization, with moderator  
112 remaining in single phase liquid during the early period of blowdown, causes a positive void  
113 reactivity feedback, e.g. Gonzales-Gonzales et al., 2014. In all cases suitable safety margins for the  
114 concerned reactors have been predicted.

115 Attempts have been made to re-define the role of the LOCA within the overall safety evaluation  
116 of water cooled reactors, also providing insights into the latest developments in the area of analyses,  
117 licensing trends and computational capabilities, OECD/NEA/CSNI, 2003, documenting a Workshop  
118 held in Zurich. Rather, the following sentence is reported from the summary of the workshop,  
119 Thadani & Laaksonen J., 2003: “... None of the participants suggested that the probability of a LBLOCA  
120 could be so high that it represents a significant contribution to the overall risk.”

121 So what remains to be investigated in the area of LBLOCA in either PWR or PHWR? Or, what  
122 can be the innovation to justify a ‘new’ publication dealing with LBLOCA? An answer to those  
123 questions is provided by the following topics which constitute the objective for the paper:

- 124 • Outlining the connection between LBLOCA and the primary system layout in both PWR  
125 and PHWR.
- 126 • Considering safety margins associated with positive void coefficient in PHWR.
- 127 • Discussing how recent research and technology achievements can be used to assess the  
128 safety of reactors designed half-a-century before (i.e. the adoption of the current BEPU  
129 approach).
- 130 • Demonstrating the importance-of and the capability-to-evaluate:
  - 131 - Three-dimensional thermal-hydraulic phenomena in the core.
  - 132 - Mechanical loads upon structures (inside and outside the vessel) generated by  
133 pressure wave propagation.
  - 134 - Coupling between thermal-hydraulics and neutron physics.
  - 135 - Nuclear fuel performance and deterministic connection with radioactive  
136 releases.
  - 137 - Long term cooling including the containment role.
- 138 • Providing recommendations for safety analyses (LBLOCA related) consistent with current  
139 technological status.

140  
141 At a time when the BEPU-based licensing of Atucha-II has been completed, GRNSPG, 2010, see  
142 also D’Auria & Mazzantini, 2009, and Petrucci et al., 2016, a LBLOCA focused re-evaluation of the  
143 (Atucha-II) performed activity constitutes the bases for the present paper. This also includes the  
144 discussion of supporting analyses and the consideration of latest literature findings which are not  
145 necessarily part of the Atucha-II licensing documents.

## 146 2. The PWR and the Atucha-II PHWR

147 The history and the bases of the PWR design are shortly revisited hereafter focusing on the  
148 safety and the origin of the LBLOCA issue, namely the logical chain:

149 <water-as- coolant-moderator> ➔ <high-pressure> ➔ <possibility-of-LOCA> ■

150 2.1. LOCA Bases for Primary Loop Design

151 Following half a century of discoveries in nuclear physics, the demonstration of sustainability  
152 of the fission reaction by E. Fermi (Dec. 2<sup>nd</sup>, 1942) constitutes a fundamental landmark for mankind:  
153 this is equivalent to the discovery of fire, achieving the ability to produce carbon steel products (the  
154 "Iron Age"), the discovery of thermal engine, or the proposition of the " $E = mc^2$ " formula from A.  
155 Einstein. The war period (WWII) plus the situation that groups of scientists in opponent Countries  
156 were working to pursue the same objective (i.e. a powerful bomb), overshadowed the importance of  
157 the discovery associated with the Fermi Pile. The unfortunate nuclear weapon explosions in 1945 did  
158 not contribute to valorize the potential strategic role of that discovery; rather, the weapon argument  
159 continues nowadays to obscure the significance of that discovery.

160 At this historical moment in the aftermath of 1942, i.e. the end of the WWII, Admiral Rickover  
161 entered the scene of the nuclear era. He looks like a sculptor who modeled the raw science material,  
162 or the graphite pile, and created a wonderful statue, or the power producing PWR: the first  
163 nuclear-powered engine and the first atomic-powered submarine, the USS Nautilus, launched in  
164 1954. All key design features of the submarine PWR are reflected in forthcoming PWR used for  
165 electricity production. An attempt is made hereafter to summarize those peculiarities.

166 In the submarine PWR, the core constituted by cylindrical fuel rods was conceived and the  
167 water was chosen as working fluid, e.g. acting simultaneously as coolant for the nuclear fuel and  
168 moderator for the energetic fission neutrons. The water was selected considering half-dozen  
169 different fluids as coolants (or even solids as moderators): this brought to the difficult-to-manage  
170 constraint of low thermal efficiency, with the (big) advantage of knowing the physical properties  
171 and the chemical interactions with other materials in the core. The selection of water fixed a  
172 roadmap for the high pressure and for the consideration of the Reactor Pressure Vessel (RPV) as the  
173 key component for the system design.

174 Other peculiarities of the submarine-resulting PWR loop can be stated as follows (see Fig. 1):

- 175 1) Avoid saturated boiling in the core to preserve the uniformity of neutron flux as much as  
176 possible.
- 177 2) Introduce steam generators to allow boiling and steam production in order to move a  
178 turbine.
- 179 3) Mutual position between core and steam generators in such a way that natural circulation  
180 can remove the decay power should main coolant pumps go out of order.
- 181 4) Piping connection with the pressure vessel at an elevation above the core and with a size  
182 (pipe diameter) to allow core cooling following the unfortunate event of pipe break.

183 The design of PWR incidentally included technological facets which made difficult its replicas;  
184 key ones are the pressure vessel itself with thick walls unsuited even for heavy industry, the  
185 sophisticate control rod drive mechanisms including related precision requirements and the need for  
186 fuel (or natural uranium) enrichment.

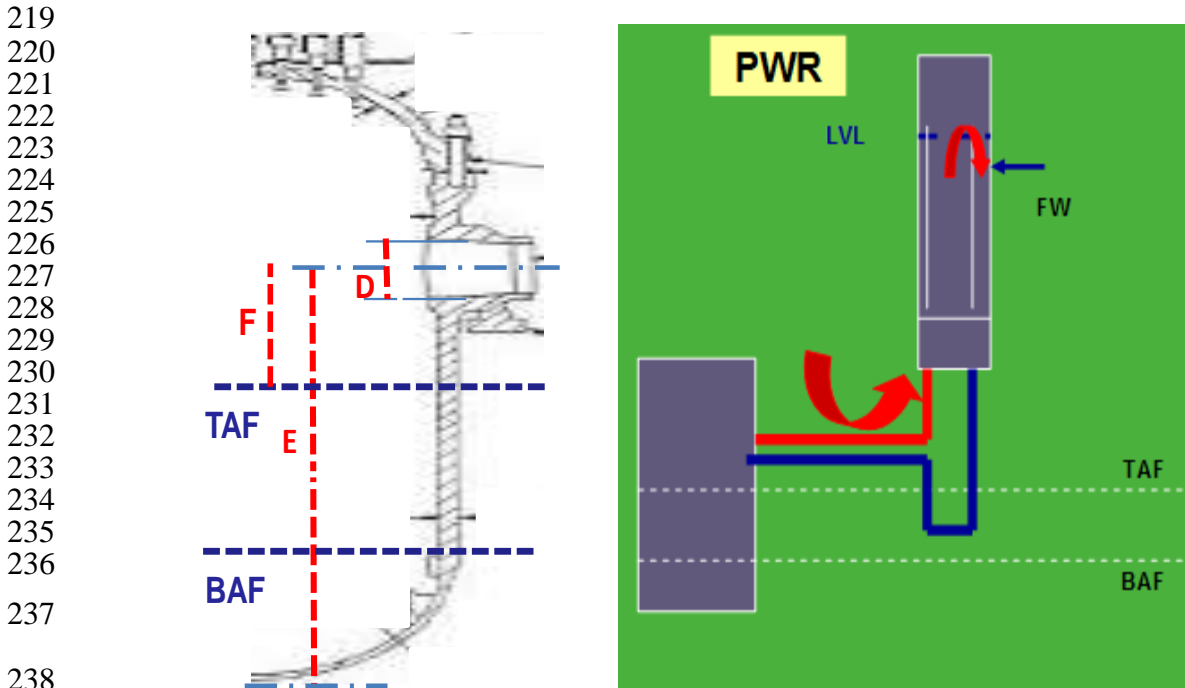
187 The key geometric and layout features of concerned Reactor Coolant System (RCS) were first  
188 decided (then planned and designed) in the 50's of the last century; later on, till current year, those  
189 features were accepted by coming generations of designers and technologists. Design ensuring  
190 safety constitutes a requirement: five related aspects connected with the LBLOCA are emphasized  
191 below.

- 192 1) Elevation of Cold Leg (CL) axis [related to the bottom of the Reactor Pressure Vessel (RPV)  
193 or, more precisely, to the elevations of the Top and Bottom of Active Fuel (TAF and BAF)].
- 194 2) Diameter of the CL pipe.
- 195 3) Mutual elevation between core and Steam Generators (SG) and overall pressure drop in SG:  
196 the elevation has a limited role in the early phase of a LBLOCA (it largely affects other  
197 LOCA situations); otherwise, the SG pressure drop may largely affect the system  
198 performance in case of LBLOCA.
- 199 4) Pressurizer role.
- 200 5) Presence of containment.

201 Sketches for the RPV and RCS of a PWR are given in Fig. 1. The relative position of CL axis and  
202 the bottom of the RPV and the TAF, 'E' and 'F' dimensions, item 1), left of Fig. 1, is such to allow

203 cooling of the core following guillotine break of the same CL pipe: the location of CL at the bottom of  
 204 the RPV (this is convenient to reduce the pressure drops in primary system) causes loss of the  
 205 injected emergency cooling liquid by gravity and the consequent impossibility to cool the core. Any  
 206 larger size for CL pipe, (D), item 2), left of Fig. 1, is convenient from the view point of minimizing the  
 207 loop pressure drops during normal operation; however, an upper limit for the diameter is fixed to  
 208 demonstrate fulfilling of Emergency Core Cooling System (ECCS) design criteria including pressure  
 209 wave propagation from break location, mechanical load of internals, rod surface temperature  
 210 excursion (maximum value and slope in a time diagram) during the early blowdown phase.

211 The layout of primary circuit is determined by the mutual position between core and SG, item  
 212 3): when the worst LOCA conditions (e.g. as far as core cooling is concerned) are determined for  
 213 DEGB in CL close to RPV, a design effort is needed to prevent the occurrence of stagnation point in  
 214 the core thus affecting the hydraulic diameter of the SG. Flow reversal in core region cannot be  
 215 avoided in case of DEGB-LOCA: fluid from PRZ, item 4), should discharge toward the core  
 216 contributing to early core cooling rather than toward the SG. Containment, item 5), shall withstand  
 217 mechanical (pipe whip, jet thrust, missiles) and thermodynamic (pressure and temperature) loads  
 218 following LBLOCA and prevent radioactivity releases to the environment according to regulation.



239 **Figure 1.** Sketch of PWR system. Left: RPV longitudinal section. Right: Primary Loop, without PRZ.

240 Design targets of Engineered Safety Features (ESF), including ECCS, ensure acceptable  
 241 radiation releases such that the containment, item 5), is not needed in principle (i.e. a properly  
 242 vented building could be enough to protect the environment). However, early designers of PWR  
 243 added the containment barrier to account for unforeseen deficiencies of the design process.

#### 244 2.1.1. The Leak before Break (LBB) Theorem

245 LBB is based upon the experimental observation that detectable fluid leakage from a large  
 246 diameter pressure pipe is expected before disruptive LOCA including double ended break, see e.g.,  
 247 Heckmann & Sievers, 2018, and Bourga et al., 2015. The LBB has a wide range of applicability in  
 248 nuclear technology, e.g. it can be used as an argument to justify the elimination of pipe whip  
 249 restraints and, definitely, for early detection of pipe rupture.

250 From a literature overview, including two mentioned papers, we synthesize the LBB theorem as  
 251 follows: *“The LBB is a detected fluid leakage including supporting analytical studies and is used as an early  
 252 alarm to scram the reactor; this may exclude the consideration of Large Break Loss of Coolant Accident*

253 (LBLOCA) from the list of events to be considered in safety analyses of individual NPP." The first sentence of  
254 the theorem can be easily endorsed; however, the last sentence is not acceptable within the present  
255 context: seismic events and unforeseen thermal stress induced corrosion erosion processes may  
256 cause a bypass of the LBB process, or a large break is not necessarily preceded by a small leakage.  
257 Specific Atucha-II related activity, [Zhang et al., 2013](#), is discussed in other parts of this paper.

#### 258 2.1.2. PWR and PHWR

259 The acronym PHWR is adopted in the literature to indicate any pressurized reactor where  
260 heavy water is used; within the PHWR class, one may distinguish the CANDU, the 'Indian'  
261 CANDU-type' and the KWU Atucha (i.e. Atucha-I and Atucha-II) NPP. The use of heavy water as  
262 moderator combined with natural uranium as fuel and the different thermal-hydraulic conditions of  
263 moderator and coolant (more details given below in relation to the Atucha-II PHWR), characterize  
264 those reactors. Following LOCA in PHWR the coolant vaporizes before the moderator and induces a  
265 fission power excursion, e.g. [Prosek et al., 2004](#). This is the effect of the so-called positive void  
266 coefficient: therefore, decrease in coolant capabilities to remove the heat generated by fission is  
267 associated to an increase of thermal power. However, the consequent fission power excursion may  
268 last a few tenths of a second with total energy generated being a small fraction of core energy during  
269 10 s of the transient, as discussed in section 4.3.2.

#### 270 2.1.3. Summary Remarks

271 LOCA and LBLOCA constitute transient events or accidents directly connected with the design  
272 of PWR (and Atucha-II type of PHWR). The consideration of those events as part of the mandatory  
273 list of DBA is challenged by the LBB theorem discussed above and, more subtly, by recently  
274 discovered nuclear fuel weakness (as mentioned in Introduction), see the review by [D'Auria et al.,  
275 2019](#). Those weaknesses leading to fuel failures primarily happen for high burn-up fuel (not of  
276 concern for PHWR) and do not exclude low burn-up fuel conditions. The consequence is that current  
277 licensing thresholds may not be fulfilled: this unavoidably introduces a challenge either to  
278 regulations (requirement not fulfilled) or to the operation of current NPP at full power (need to  
279 dramatically reduce the nominal power).

280 Summary-conclusions from the discussion above are: (a) design related motivations to keep  
281 LBLOCA as a key accident in safety analyses have been re-stated; (b) a relaxation in the application  
282 of current licensing criteria and the (obvious) full consideration of the role of containment are  
283 needed for licensing, [D'Auria et al., 2019](#).

#### 284 2.2. The Atucha-II Peculiarities

285 The central nuclear Atucha II (CNA-II) is a two-loop, 745-MWe, pressurized heavy water  
286 reactor (PHWR) nuclear power plant (NPP), operating in Lima, Argentina. The reactor is cooled and  
287 moderated by heavy water, see sketches in Figures 2 and 3 and summary data in Table 1, [Bonelli et  
288 al., 2014](#), and [Mazzantini et al., 2018](#).

289 The core consists of 451 vertical natural uranium fuel assemblies located in the same number of  
290 coolant channels. The coolant channels are surrounded by the moderating heavy water, which is  
291 enclosed in the moderator (MOD) tank. For fission reactivity reasons the moderator is maintained at  
292 lower temperature than the reactor coolant. This is accomplished by the MOD system, which  
293 extracts the moderating water from the MOD tank, cools it in the MOD coolers and feeds it back to  
294 the MOD tank.

295

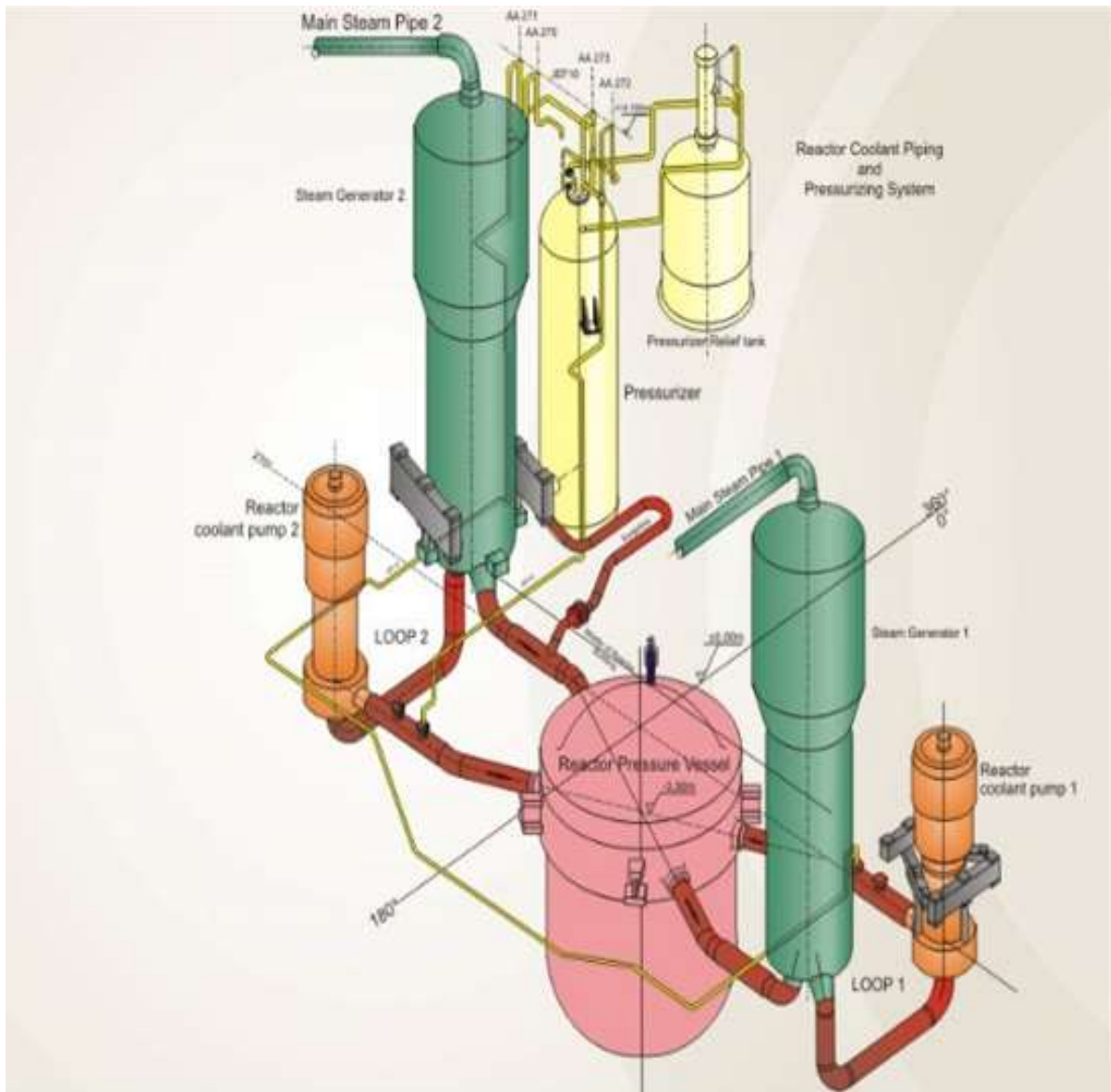


**Figure 2.** Sketch of the primary system, reactor cooling, of Atucha-II.

296  
 297  
 298  
 299  
 300  
 301  
 302  
 303  
 304  
 305  
 306  
 307  
 308  
 309  
 310  
 311  
 312  
 313  
 314  
 315

During full-load operation, 95% of the total thermal power is generated in the fuel, and the remaining 5% in the MOD, because of the neutron moderation. Additionally, approximately 5% of the thermal power is transferred from the coolant to the MOD through the coolant channels walls, due to the temperature difference between the systems.

The heat removed from the MOD is used for preheating the steam generators (SG) feed water. The reactor coolant system and the MOD system are connected by pressure equalization openings of the moderator tank closure head. Therefore, the pressure differences in the core between the primary coolant and MOD systems are comparatively small, which results in the thin walls for the coolant channels. This allows attaining a high burn-up. Furthermore, the connection between the reactor coolant system and the MOD system permits the use of common auxiliary systems to maintain the necessary water quality.

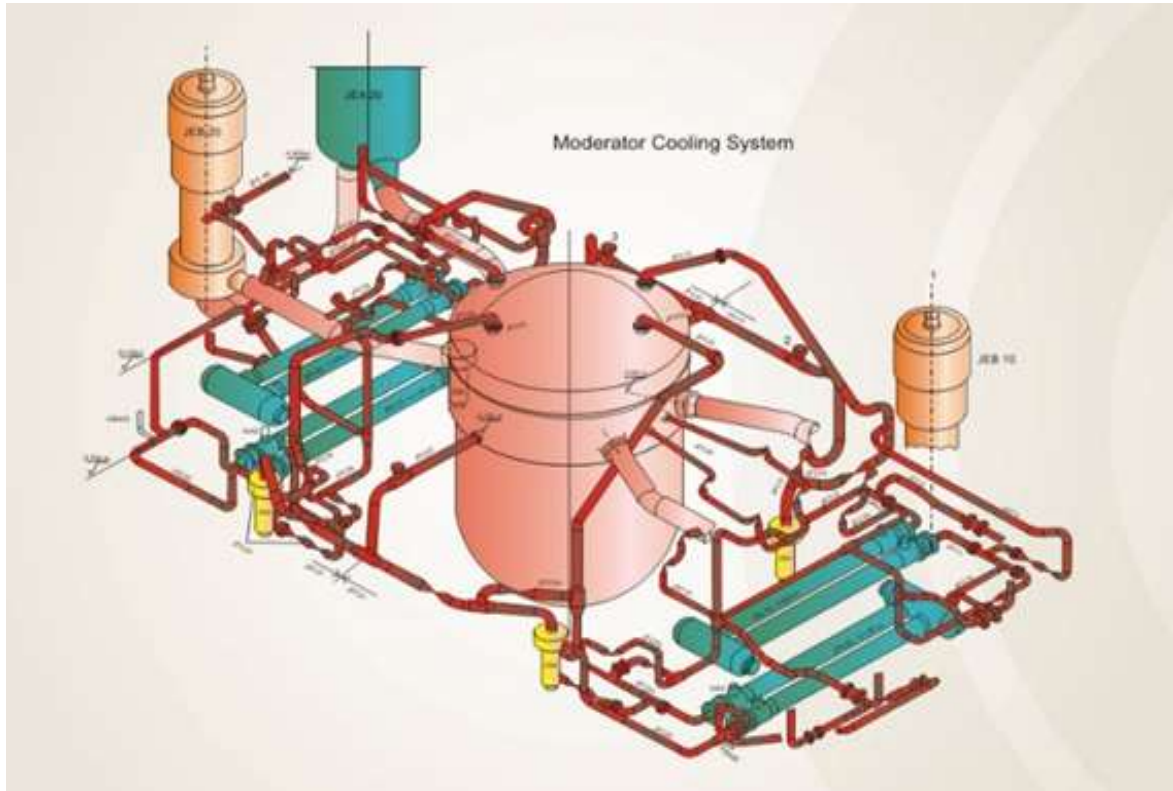


**Figure 3.** Sketch of the primary and moderator cooling systems for Atucha-II.

316

317

318

319

320

321

322

323

324

325

326

327

328

329

330

331

332

333

334

The primary system is structured similarly to a PWR (light water reactor) and consists of two identical loops, each comprising a steam generator, a reactor coolant pump, and the interconnecting piping, as well as one common pressurizer.

The MOD system consists of four identical loops operating in parallel. Each loop comprises MOD cooler, pumps, and the interconnecting lines with valves. The moderator system performs various functions depending on the reactor-operating mode. During normal operation the moderator system maintains the moderator at a lower temperature than that of the reactor coolant. The moderator leaves the top of the moderator tank, flows to the moderator pumps, pumped there through the moderator coolers, and flows back to the bottom of the moderator tank. The heat transferred in the moderator coolers is used to preheat the steam generator feed water. For residual heat removal, the moderator system is switched over to the residual heat removal position by means of the moderator valves. Under this operation mode, the moderator is extracted from the bottom of the moderator tank by the moderator pumps and fed into the cold/hot legs of the reactor coolant loops. During emergency core cooling, the moderator system serves as a high-pressure core cooling system. The emergency core cooling function is similar to that of the residual heat removal. The residual heat removal chain connected to the moderator coolers during emergency core cooling is the same as during residual heat removal in nominal operation.

335

### 2.2.1. System Complexity

336

337

338

339

340

341

342

Having the aim to provide an insight into the comparison between PWR and PHWR, a summary of technological complexities for the two systems can be found in Table 2.

The adoption of natural uranium as fuel constitutes an advantage (or a lack of complexity) for the PHWR which otherwise needs the costly heavy water as moderator. The continuous (daily) fuel replacement and the consequent need for fuel loading and un-loading machine constitute a complexity for the PHWR. The difficulty to prevent mixing between heavy and light water (thus losing the high valued heavy water) imposes heavy water as a coolant for PHWR. The need to keep



343 moderation function imposes (relatively) low temperature for the moderator and therefore a  
 344 separate loop.

345 **Table 1.** Atucha-II PHWR overall data.

QUANTITY	VALUE	NOTES
Net power generation	745 Mwe	
Thermal power	2160 Mwth	Including core and moderator cooling
N of cooling channels	451 (-)	37 fuel rods of natural uranium – cylindrical channels
Coolant and Moderator	D2O	
Power to steam generators	1954.5 Mwth	Thermal power transferred to the 'steam cycle' = 2174.5 Mwth (including main coolant pump power).
Power to moderator coolant	220 Mwth	
No of coolant / moderator circuits	2 / 4	2 HEX per SG to cool the moderator
Circulation flow, core / moderator	10300 / 890 kg/s	Equivalent to $\approx 28 / 2$ kg/s per channel
Pressure at vessel inlet/outlet	12.25 / 11.53 MPa	For both coolant and moderator
Coolant temperature	280 / 311 °C	Vessel inlet / outlet (→ about 10 K sub-cooling)
Moderator temperature	189 / 204 °C	Vessel inlet /outlet (selected operational condition)
Average moderator temperature	170 / 220 °C	Normal/maximum value (design expected range)
Pressure at steam generator outlet	5.49 MPa	
Total steam flow	956 kg/s	
Power density & max LHGR	12 kw/l & 45 kw/m	(power density in PWR is 100 kw/l)
SIP & ACC injection ports	4	Two in each CL and HL
Containment pressure / volume	0.7 bar / 50 E3 m <sup>3</sup>	Spherical pressure boundary design values

346  
 347 Control Rod Drive Mechanism (CRDM) in PHWR is designed having lower mechanical  
 348 precision requirements than in the case of PWR. This advantage (for PHWR) is counterbalanced by  
 349 the need of having a fast boron injection system capable of injecting boron into the moderator in less  
 350 than one second following a demand (e.g. to deal with positive void coefficient after LBLOCA).

351 In relation to both PWR and PHWR, a Reactor Pressure Vessel (RPV) is needed (internal  
 352 diameter about 4.5 and 7.0 m, respectively): the RPV size is larger in PHWR per unit power owing to  
 353 the lower power density in the core (about 12 and 100 kw/l, respectively); however wall thicknesses  
 354 are comparable for RPV in PWR and PHWR owing the lower nominal pressure in PHWR than in  
 355 PWR.

**Table 2.** Summary of PWR and PHWR system complexities.

No	SYSTEM COMPLEXITY	PWR	PHWR (Atucha-II)	NOTES (complexity connected with, e.g.)
1	RPV	X	X	Wall thickness
2	CRDM	X		Precision
3	Fuel Enrichment	X		Enrichment
4	Heavy Water		X	Availability and cost
5	Boron Injection System		X	Time of actuation following demand
6	Load/Unload machine		X	Design function
7	Moderator loop		X	
8	I&C	X	X	

### 3. The LBLOCA Elements (PWR & PHWR)

Several LOCA-related documents are available from literature (and web): the difficulty to provide innovative information has already been recognized. Nevertheless, the consideration all together of aspects related to (a) pressure wave propagation, (b) fluid-dynamics, (c) heat transfer, (d) chemical reaction, (e) mechanical loads, (f) neutron physics, (g) nuclear fuel performance, (h) containment, and (i) sump recirculation (including debris), may imply an innovation.

The application of complex codes is needed to discuss items (a) to (i): this requires the demonstration of capabilities for the numerical tools and the qualification (or V&V) for the generated calculation results, e.g. *D'Auria & Galassi, 1998*; unavoidable uncertainty evaluation is also involved, *IAEA, 2008*. Physical aspects reflecting current understanding and assuming the availability of suitable computational tools are discussed in sections 3.1 to 3.6 (general level) and 4.1, 4.2 (Atucha-II specific).

Sensitivity studies are needed in advance, i.e. preliminarily to 'final deterministic analyses', in order to characterize the boundary conditions for LOCA (as well as for any other transient part of DBA) which cause the largest challenge to safety margins. Examples of targets for preliminary sensitivity studies are (search for):

- break location (along the primary loop piping) which causes the largest PCT;
- break location which causes the highest containment pressure;
- break size at a given location, which results in the highest PCT;
- break location which results in the highest load on RPV internals or on containment structures distinguishing between pressure wave (impulse type of load) and fluid-dynamic (static type of load) origin;
- configuration of ECCS (e.g. when two out of four accumulators are assumed to actuate, selection of the least effective ones) which causes the highest PCT;
- break size and location which result in the highest Fission Power Peak (FPP) when positive void coefficient is part of the core design.

Typical outcomes from preliminary sensitivity studies performed in relation to Atucha-II LOCA (discussed in section 4) are given in Figs. 4 and 5.

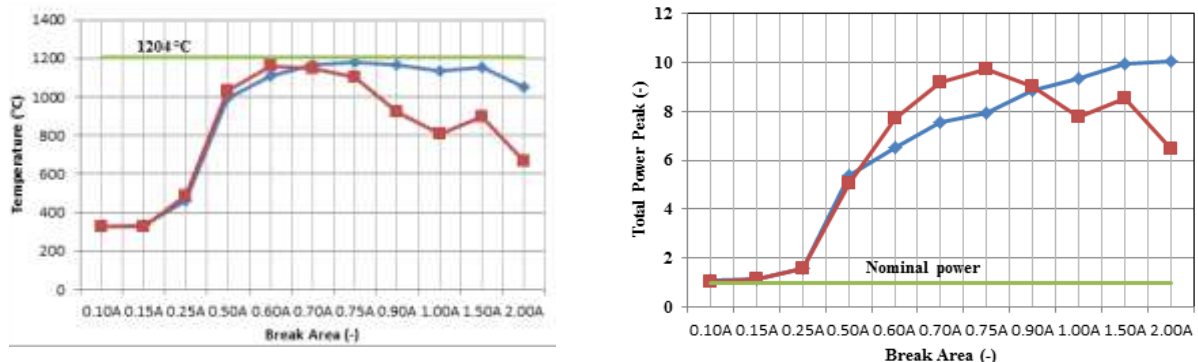
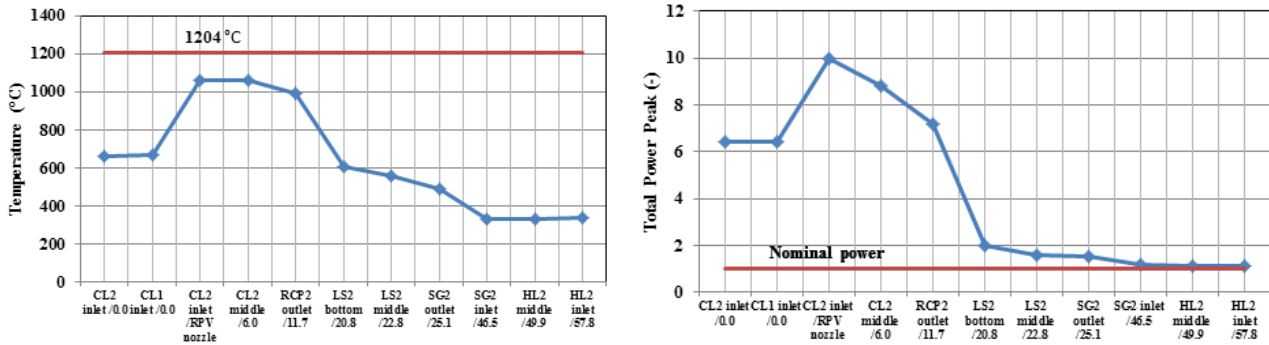


**Figure 4.** Sensitivity studies from Atucha-II LBLOCA: PCT (left) and FPP (right) vs break area; for each diagram two curves obtained from different (qualified) nodalizations.



387 **Figure 5.** Sensitivity studies from Atucha-II LBLOCA: PCT (left) and FPP (right) vs break location [in  
 388 the horizontal axis: break location expressed as the distance from RPV-CL connection (m)].

389 The following can be deduced from the analysis of the diagrams:

- 390 ➤ A range of break sizes for PCT must be considered (starting from 0.4A up to 2A where A is
- 391 the cold leg cross section area and 2A = DEGB);
- 392 ➤ The worst break size as far as FPP is concerned is 2A;
- 393 ➤ The worst break location (either PCT or FPP) is in the cold leg at the outlet of the RPV.

394 The evaluation of other challenges (not shown here) considering above bullet items confirms  
 395 the importance of the DEGB. However, a larger number of ‘final deterministic analyses’ (i.e. in  
 396 addition to the DEGB LBLOCA) are needed to systematically consider the worst situation for each  
 397 concerned safety margin (not further discussed here).

398 *3.1. The Early Blowdown – the 1<sup>st</sup> Period: the (Fast) Dynamic Effects*

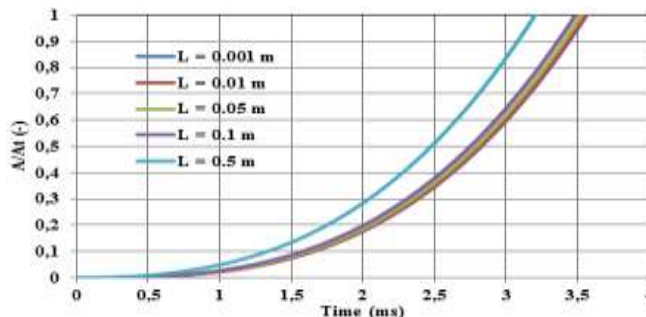
399 Considered topics are relevant to both PWR and PHWR with noticeable exception of ‘fission  
 400 power excursion’ and ‘fast boron injection’ which apply to PHWR (time duration is a few seconds).

401 *3.1.1. Break Opening Time (BOT)*

402 Intuitively BOT affects the depressurization wave formation at the break, namely its amplitude,  
 403 and, consequently generated loads. Fracture mechanics, corrosion-erosion, presence of weld,  
 404 geometric or material discontinuities, material plasticity, local stress-strain status, detectable defect  
 405 and compressibility of the pressurized fluid constitute (a minimum set of) elements affecting the  
 406 BOT. Attempts to estimate BOT are discussed in the literature, e.g. [Baum, 1984](#), and [Bhandari &](#)  
 407 [Leroux, 1993](#). Namely, a theoretical approach is proposed by Baum (also reported by [Ylonen, 2008](#))  
 408 ending-up with the formula, see diagram in Fig. 6:

$$A = \frac{2P_0 \mu_p t^3}{3m} + \frac{P_0 L t^2}{m} \quad (1)$$

409 where, A = the actual flow area, t = time, P<sub>0</sub> = initial internal pressure, L = initial defect length, m = mass per unit area of the  
 410 pipe wall and  $\mu_p = (\sigma_y / \rho_s)^{1/2}$  = ductile fracture propagation velocity [with  $\sigma_{ys}$  = yield stress at prevailing strain and  $\rho_s$  =  
 411 density of pipe material].



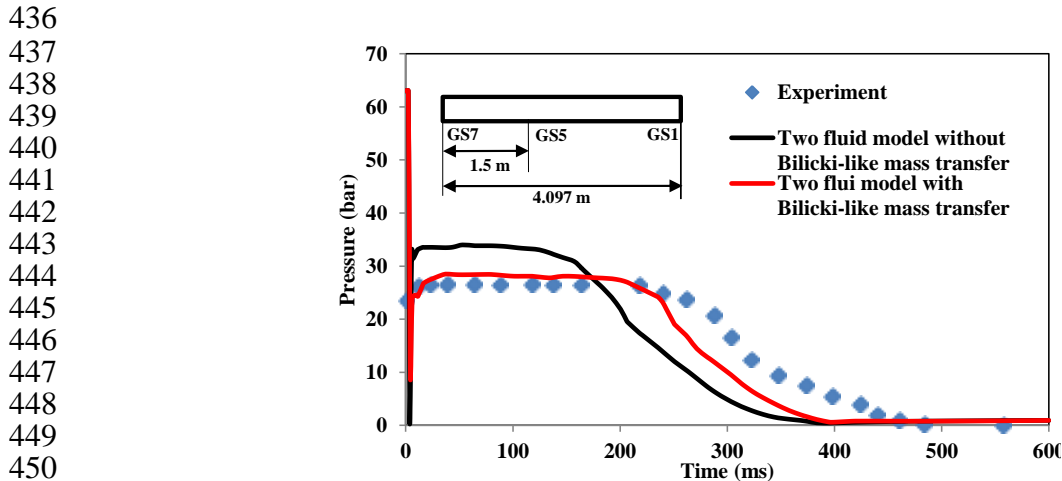
420 **Figure 6.** Break flow area versus BOT for different initial defect length [L], derived from [Baum, 1984](#).

421 The overall (silly) conclusion from reported references can be summarized as follows in the case  
 422 BOT is estimated for a large pipe in the conditions of cold legs in a PWR: about 100 m-s BOT is  
 423 expected, however lower values cannot be excluded.

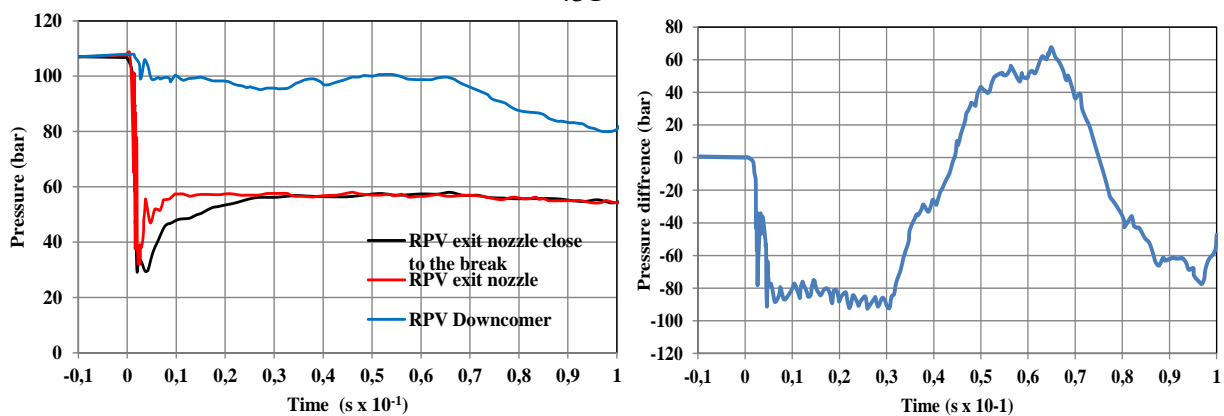
424 In the case of licensing analyses, where the evaluation of pressure wave effect is excluded,  
 425 typical value used for BOT corresponds to one time-step of the code-calculation (time step has a  
 426 typical value in the range 1 – 10 m-s). Additional details are given in section 4.3.1 related to  
 427 Atucha-II calculations.

### 428 3.1.2. Depressurization Wave Propagation

429 Following the start of rupture occurrence (or break opening), a (negative) pressure wave  
 430 (sometimes called a rarefaction wave) propagates from the break towards the RPV and in the  
 431 opposite direction, towards the Main Coolant Pump, in the case of a LOCA in a PWR. Selected  
 432 experimental and data and in one case results of calculation are given in Fig. 7: Edwards, [Edwards &  
 433 O'Brien, 1970](#), and HDR, [Wolf, 1982](#), experiments are given together with results of calculations  
 434 performed by [Lochon et al., 2017](#), in the case of Edwards experiment (see also discussion related to  
 435 Fig. 9 below).



451



452

453 **Figure 7.** Pressure wave propagation. Upper diagram: comparison between measured and calculated  
 454 data for Edwards pipe experiment ([Edwards & O'Brien, 1970](#), and [Lochon et al., 2017](#)), GS7 location.  
 455 Lower diagrams are related to HDR tests ([Wolf, 1982](#)): left: absolute pressure in exit nozzle and in  
 456 RPV downcomer; right: pressure difference between outside and inside the barrel [ $P_{\text{outside}} - P_{\text{inside}}$ ].

457 The following can be derived from the analysis of the figure, assuming a BOT in both cases of  
 458 the order of 2-5 m-s, with rupture occurring in special membranes properly designed:

- 459 ✓ The pressure wave moves (starting from the break) at a velocity close to the sound speed.
- 460 ✓ The Amplitude of the Pressure Wave is a complex function of (a) BOT including time  
 461 derivative (APW larger for smaller BOT), (B) sub-cooling of the fluid (APW larger for high

462 subcooling), (c) size of the system compared with break area (APW smaller for larger sizes),  
463 (d) compressibility of the fluid (e.g. APW decreasing when passing in the pressurized  
464 reservoir from subcooled liquid to two-phase mixture), (e) system geometry (e.g.  
465 dimensions of a nozzle connected with a reservoir, and presence of internals).  
466 ✓ The pressure wave induces impulse and cyclic loads (soliciting fluid-structure interactions)  
467 upon internals as can be inferred from the bottom right diagram.  
468 ✓ Occurrence of a double critical section for TPCF (or two TPCF locations) can be derived  
469 from the bottom left figure.  
470 ✓ Current (Lochon et al., 2017) 'low' predictive capabilities of pressure wave models,  
471 following fast depressurization, can be seen from the upper diagram. This is true,  
472 notwithstanding good predictive capabilities demonstrated in different situations, e.g. case  
473 of pressure wave originated by closure of turbine inlet valve, Bousbia Salah et al., 2004.

### 474 3.1.3. Two-Phase Jet, Jet-Impingement and Thrust

475 Break formation implies fluid jet formation and interaction with surroundings. The jet can be a  
476 cylinder of the same diameters of the exit pipe when high subcooled flow is concerned, e.g. ambient  
477 temperature liquid flowing out of a reservoirs pressurized by gas. In the case of RPV at  
478 thermal-hydraulic conditions of a nuclear reactor a conic or a paraboloid jet forms depending upon  
479 void fraction at pipe outlet: from low to high void fraction the bounding jet shape with the jet axis as  
480 center-line, moves from paraboloid to cone, see e.g. D'Auria & Vigni, 1981, and Celata et al., 1986;  
481 the last authors also measured the pressure inside the jet.

482 Hereafter the attention is focused to the load caused by the jet acting upon both any hypothetic  
483 structure outside the RPV and upon the vessel supports. The load (F) can be expressed as:

$$F = KP_0 A \quad (2)$$

484 where  $P_0$  = reservoir pressure;  $A$  = break flow area;  $K$  = coefficient discussed below for various cases.

485  
486 In the case of a jet impinging upon a flat plate orthogonal to the jet axis, a  $K$  value in the range  
487 1.0 – 1.2 is measured at a distance between the plate and the exit area cross section plane in the order  
488 of a few pipe diameters, Vigni & D'Auria, 1979, and Yano et al., 1982. The value is affected (other  
489 than by the thermal-hydraulic conditions inside the reservoir, namely by the void fraction at the  
490 break section) by the distance of the plate from the break; the value  $K=2$  can be characterized as an  
491 upper limit for  $K$ .

492 The thrust upon RPV supporting frame shall be considered as the sum of the 'jet reaction force'  
493 and the spring type mechanical force associated with the mechanical energy stored into the piping  
494 material; in the case of a RPV ending up with the jet exiting nozzle, the spring force depends upon  
495 the nozzle length and flow area, the wall thicknesses and the size of the possible flange at the pipe  
496 end. The measured value for  $K$  has been measured in the range 1.0 – 2.0, Vigni & D'Auria, 1979,  
497 and D'Auria & Vigni, 1981, (see also Kurihara et al., 1987), with a maximum theoretical value  $K=4$ .  
498 Impulse type of load occurs during the first few m-s after break opening and are consistent with  $K$   
499 values larger than about 1.2.

### 500 3.1.4. Pipe Whip and Break-Generated-Missiles

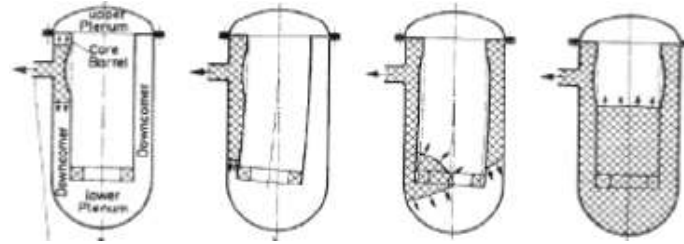
501 Pipe whip and missile generation are associated with break opening: related phenomenology  
502 occurs at a time scale in the orders of 0.1 -1.0 s.

503 Without entering into details like ovalisation of a pipe or complex elastic-plastic formulations  
504 Reid et al., 2011, and experimental data Kurihara et al., 1987, the pipe whip investigations end up  
505 with the design of suitable restraints or in the demonstration that pipe movements do not impact the  
506 integrity of safety components and safety functions.

507 Current status and issues related to missiles are discussed by Ranjan et al., 2014: ensuring the  
508 resistance for structures and components hit by missiles constitute typical objectives for the analyses.  
509 In relation to both cases of pipe whip and generated-missiles, assuming suitable safety  
510 demonstration according with mentioned targets, there is no further impact with LBLOCA  
511 evolution and no further discussion hereafter.

512 3.1.5. Load on RPV Internals

513 The depressurization wave generated at the break enters (namely in the case of a PWR) the  
 514 annular space between the reactor vessel and the core barrel, then it travels down to the lower  
 515 internals as it wraps around the barrel. This is illustrated in Fig. 8 taken by [Krieg et al., 1977](#), and  
 516 later on (widely spread picture) by [Hosford et al., 1981](#) (USNRC NUREG-0609). The  
 517 depressurization wave, depending upon its amplitude and the sub-cooling of the encountered fluid,  
 518 may generate voids with a delay of the order of m-s after its passage. This causes complex Fluid  
 519 Structure Interaction (FSI), [Mahmoodi et al., 2019](#), see also [Vigni et al., 1978](#), for experimental data in  
 520 simple geometry blowdown. Following the definition of FSI, mutual interaction occurs among  
 521 moving of fluid, void formation and motion of internals (see also Fig. 8).



530 **Figure 8.** Propagation of depressurization wave from the break (shaded region is at low pressure),  
 531 [Krieg et al., 1977](#).

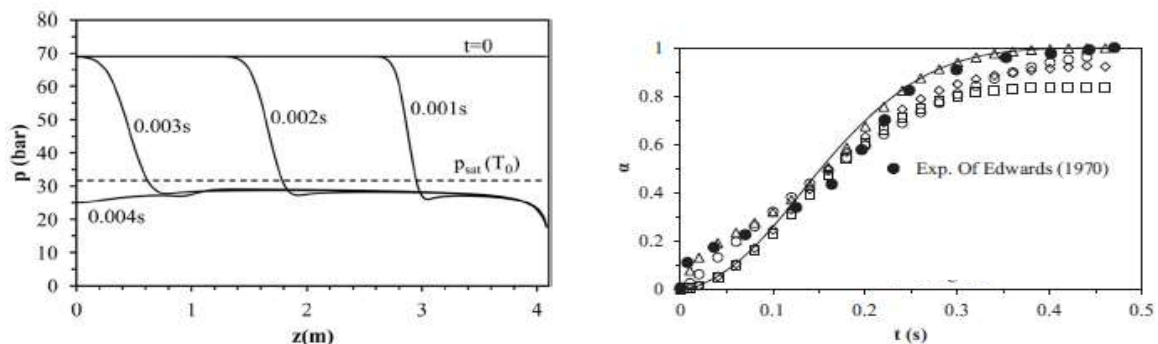
532 The capability to withstand blowdown loads by the Control Rod Drive Mechanisms (CRDM) in  
 533 the upper plenum of a PWR is discussed and demonstrated as far as possible, by [Krieg et al., 1982](#).

534 3.1.6. Flashing in RPV

535 The effect of a depressurization wave is to create voids (vaporization due to depressurization in  
 536 the phenomena list, [Aksan et al., 2018](#)) in a subcooled liquid, provided an amplitude such to create a  
 537 pressure lower than the pressure corresponding to the local saturation temperature. The delay in  
 538 void formation can be estimated as in the order of milliseconds, see e.g. [Nouri-Borujerdi & Ghazani,  
 539 2018](#); in some situations measured delays between pressure decrease and void formation can be as  
 540 low as a fraction of one m-s as reported by [Faucher et al., 2000](#). An effect of neutron flux upon  
 541 nucleation and void formation during blowdown is reported in the literature, e.g. [Kendoush, 1989](#).

542 A correlation between pressure wave and void fraction / vaporization (and vaporization rate)  
 543 resulting from flashing can be deduced from the [Edwards & O'Brien, 1970](#), experimental data, Fig. 9:  
 544 the consideration of data in Fig. 7 (upper diagram) allows observing how void formation (flashing)  
 545 contributes in keeping the system pressure nearly constant during the period 10 – 280 m-s.

546 Flashing in core region causes lack of moderation and immediate termination (consistently with  
 547 the arrival of the pressure wave from the break) of the fission reaction. Flashing in lower and upper  
 548 plenum at different times interact with core flashing and flow reversal as discussed in next section.  
 549



550 **Figure 9.** Propagation of depressurization wave and void formation, [Edwards & O'Brien, 1970](#), test  
 551 as reported by [Nouri-Borujerdi & Ghazani, 2018](#), together with results of prediction models.

552 3.1.7. Flow Reversal in Core Region

553 The change in flow direction from nominal conditions is characterized as flow reversal and may  
554 occur at any point in the core: flashing and flow stagnation associated with pressure wave  
555 propagation together with flow inertia and MCP operation, determine flow reversal. This happens  
556 during both the 1<sup>st</sup> and the 2<sup>nd</sup> LOCA period, typically leading to flow-rate oscillation primarily  
557 during the 2<sup>nd</sup> period.

558 The origin of the flow reversal is the 'pressure sink' (negative term) which establishes at the  
559 break and is not (sufficiently) balanced by the initial flow inertia and by the flow momentum coming  
560 from the operation of the pumps in the intact loops (positive terms). Flow reversal is reported to  
561 occur during a calculated LBLOCA transient at 3 s after the break occurrence, [D'Auria & Galassi, 2017](#);  
562 more details are given in Section 4.2.3.

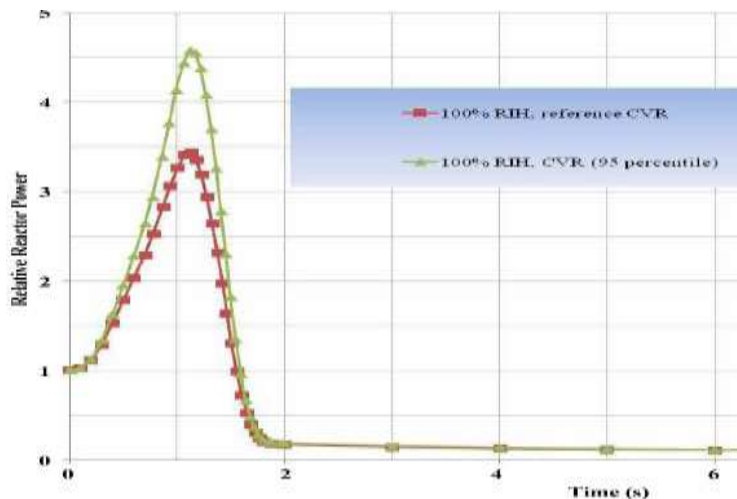
563 3.1.8. Neutron Physics and Fission: Reactivity Coefficients and Power Excursion

564 PWR case: all neutron fission reactivity coefficients are solicited during LOCA. However the  
565 arrival into the core of the depressurization wave generated at the break a few m-s after the  
566 occurrence, creates enough void such to stop the fission reaction; in other terms decay heat becomes  
567 the only source of energy in the core independently upon the actuation of scram rods which also are  
568 immediately called into operation. This is also valid when high boron concentration, at the  
569 beginning of core life, causes a positive moderator temperature coefficient: the effect of void  
570 formation (in case of LBLOCA) overpasses the effect of expelling a (highly) neutron absorbing  
571 moderator from the core region.

572 PHWR case: the moderator and coolant are at different temperature during nominal operating  
573 condition; therefore the depicted scenario for PWR does not apply. Early coolant voiding following  
574 LBLOCA deprives the core of a neutron absorbent material and a fission power excursion is  
575 unavoidable. Furthermore, the rate of increase in reactor power in a heavy water moderated reactor  
576 is inherently limited by its relatively long prompt neutron lifetime (about 40 times longer than that  
577 in a light water moderated reactor), so that the reactor period is much longer and the rate of rise in  
578 power and enthalpy is much slower, [Popov & Snell, 2012](#).

579 A typical fission power excursion calculated for CANDU reactors with different assumptions  
580 adopted for deriving the void coefficient is reported in Fig. 10, [Kastanya et al., 2013](#).

581  
582  
583  
584  
585  
586



587  
588  
589  
590  
591  
592  
593  
594

595 **Figure 10.** Fission power excursion during LBLOCA in CANDU, [Kastanya et al., 2013](#).

596 3.1.9. Boron Injection

597 In the case of the Atucha-II a special Boron Injection System is installed which is capable of fast  
598 injection of boric acid suitable to limit the power excursion expected as a consequence of the positive  
599 void reactivity coefficient, e.g. [Moretti et al., 2018](#). More details are given in sections 4.2 and 4.3.2.

600 3.2. *The Blowdown 2<sup>nd</sup> Period, the 1<sup>st</sup> PCT – up to Accumulator Actuation*

601 A picture has been given in section 3.1 of key phenomena occurring soon after the break  
602 opening (a few seconds) following LOCA in PWR and PHWR, i.e. pressure wave dominated effects.  
603 What happens during a few tens of seconds till the intervention of accumulators is discussed  
604 hereafter: i.e. emphasis given to core heat transfer and fast depressurizing two-phase mixture  
605 evolutions.

606 3.2.1. The TPCF

607 TPCF has a strong impact upon overall system performance, namely core cooling, during a  
608 PWR LOCA. A synthesis of TPCF related ideas and modeling is well beyond the framework of the  
609 present paper; nevertheless a few statements are provided below to connect with sections 3.1 to 3.6:

- 610 a) TPCF is a recognized 'leading phenomenon' in case of LOCA, see e.g. [Aksan, 2017](#).
- 611 b) Break flowrate (or TPCF) directly affects depressurization rate, pressure distribution in the  
612 loop, mass and energy lost from the break and containment pressurization.
- 613 c) TPCF is strongly affected by geometry other than by fluid conditions that establish at the  
614 break: sharp edges, crack shapes, L/D ratio in nozzle, valve geometry (e.g. fluid discharge  
615 valves) strongly affect the phenomenon and multiple TPCF section may occur  
616 simultaneously, or TPCF location may move during a transient.
- 617 d) Notwithstanding experimental researches and modelling efforts since the 60's of previous  
618 century, predictive capabilities for TPCF need improvement: discrepancies between  
619 measured and calculated values can be as large as 30% of the measured value; current model  
620 validation procedures appear inadequate specifically in the case of TPCF, as discussed by  
621 [D'Auria & Lanfredini, 2018](#).
- 622 e) Nucleation sites: the impact of nucleation sites in predicting bubble size is discussed by  
623 [Nigmatulin et al. 1987](#).
- 624 f) Attention currently drawn by the 'TPCF issue' can be derived by [Jo et al., 2018](#), and  
625 [Hamouda et al., 2018](#), who point out the importance of considering two pressures in  
626 modeling [*Models that do not account for the pressure differential across the vapor-liquid interface*  
627 *will significantly under-predict the rate of vapor growth*]

628 3.2.2. The Flow Stagnation

629 Depending upon the MCP and overall flow inertia in the primary loop, flow stagnation (or  
630 nearly zero fluid velocities) may occur during the 1<sup>st</sup> and the 2<sup>nd</sup> period: in the former case, the  
631 pressure wave formation at the break and the propagation in two opposite direction may generate a  
632 potential flow stagnation in the loop location where the two pressure waves come across; in the  
633 latter case two-phase (primarily) pressure drop balance along the two sides of the loop caused by the  
634 break, generate the flow stagnation. The flow stagnation, or better the flow stagnation region; (a) has  
635 a dynamic nature and may continuously migrate as a function of time; (b) implies very low fluid  
636 velocities and therefore very low heat transfer coefficients.

637 A suitable design/repartition of pressure drops along the primary loop may ensure that flow  
638 stagnation does not occur in the core; large pressure drops in primary side of steam generator may  
639 facilitate stagnation region inside the U-tubes. This ensures more fluid in the core following upper  
640 plenum flashing and pressurizer draining in case of LBLOCA.

641 3.2.3. CHF Occurrence, Pellet Stored Thermal Energy and the (1<sup>st</sup>) PCT

642 Background considerations given for TPCF apply here: CHF is a widely studied phenomenon  
643 topic of textbooks, e.g. [Collier, 1975](#), and highly impacting LBLOCA. A few notes are provided  
644 below:

- 645 1) Accurate knowledge of CHF is needed in order to establish safety margins during nominal  
646 core operation: this allows achieving high linear power which directly impacts (see below)  
647 the occurrence of CHF following LOCA.
- 648 2) Nuclear fuel designers and suppliers adopt specific experiment-derived correlations for  
649 CHF suitable to optimize fuel performance and to demonstrate safety margins.



- 650 3) Spacer grids (number and types) other than fuel bundle equivalent diameter and local  
651 thermal-hydraulic parameter values, e.g. [Aksan et al., 2001](#), affect the CHF occurrence in  
652 nominal and transient conditions.
- 653 4) Notwithstanding the large number of ('more or less') empirical correlations to determine  
654 CHF, the most widely used approach, namely for transient analyses, is based upon the  
655 so-called Groeneveld and Kirillov look-up tables, [Groeneveld et al., 1996](#), which directly  
656 make reference to several ten thousands experimental data points.
- 657 5) Following LBLOCA, CHF may occur either immediately after the break as the result of  
658 flashing generated by depressurization wave or a few seconds later due to flow reversal and  
659 low fluid velocity: both situations may occur in different regions of the core at different  
660 times.

661 CHF occurrence generates (the 1<sup>st</sup>) rod surface temperature excursion: slope and values for the  
662 temperature excursion, including PCT, are primarily determined by the fuel pin linear power ( $q'$  or  
663 Linear Heat Generation Rate, LHGR, [kw/m]) in nominal conditions: scram time (originated by  
664 moderator voiding, section 3.1), flashing (core, upper and lower plenum) and flow reversal affect the  
665 post dry-out heat transfer, [Hewitt et al., 1992](#), and the instantaneous temperature value. Presence of  
666 oxide and crud may affect rod surface temperature values up to a couple hundred Kelvin. The 1<sup>st</sup>  
667 PCT, also called blowdown PCT, is terminated by an early core rewet (next discussed item) or  
668 continues, with a reduced slope, giving rise to the 2<sup>nd</sup> PCT (section 3.3).

#### 669 3.2.4. The early Core Rewet

670 Following CHF and the initial rod surface temperature excursion, a turnaround for the  
671 temperature (reported as a function of time since the transient start) may occur well before the  
672 actuation of accumulators and has been measured in LOFT facility, [Brittain & Aksan, 1990](#); the  
673 turnaround may end-up to a complete local quench, so called early core rewet, or to a (small early)  
674 decrease in temperature value, e.g. [Queral et al., 2015](#). Pump characteristics, flashing and droplet  
675 entrainment and eventually flow from pressurizer are at the origin of partial or complete early core  
676 rewet.

#### 677 3.2.5. The Depressurization Rate

678 The primary coolant pressure decrease and pressure decrease rate (depressurization  
679 characteristics) constitute essential parameters for blowdown and LOCA. Depressurization  
680 characteristics affect and are connected with mass loss and time of actuation of accumulators or  
681 accumulator design pressure: early actuation of accumulators (or high design pressure) may cause  
682 too much of injected mass lost to the break; late actuation of accumulators (or low design pressure)  
683 may cause too high rod surface temperature. Therefore, the knowledge of depressurization  
684 characteristics is essential (also) before the actuation of accumulators.

685 Typical average values for depressurization rate from break opening till the concerned time are  
686 1-3 MPa/s, 1 MPa/s and 0.5 MPa/s, for the 1<sup>st</sup>, the 2<sup>nd</sup> and the 3<sup>rd</sup> blowdown period, respectively  
687 (sections 3.1 to 3.3), see e.g. [Queral et al., 2015](#), and [D'Auria & Galassi, 2017](#).

#### 688 3.2.6. The Containment Pressure Peak

689 Depressurization of primary system corresponds to pressurization of containment, full pressure  
690 type in PWR, see e.g. [OECD/NEA/CSNI, 1999](#), and [Noori-Kalkhoran et al., 2016](#). Following pipe  
691 whip, jet impingement, thrust on RPV supports and possible missiles during the first LOCA instants,  
692 pressure and temperature loads in containment are created by the discharging two-phase flow. Peak  
693 pressure is expected during the time interval 10-20 s after break occurrence with a value 0.35 – 0.55  
694 MPa, depending upon the reactor unit, the break location and the assumptions about the accident  
695 progression including mitigation measures. Hydrogen management is expected inside containment  
696 (see also section 3.3).

697 Containment constitutes the ultimate (robust, not to be overpassed) barrier against the massive  
698 release of fission products into the environment.

699 3.3. *The Late Blowdown (3<sup>rd</sup> period), the 2<sup>nd</sup> PCT – the Refill, up to LPIS Actuation*

700 The intervention of accumulators, typically at a primary pressure of 4.0 MPa at around 30 s,  
701 fixes the time when refill and recovery actions for core cooling start. The minimum mass inventory  
702 for the primary system (in the order of 10% of initial value) occurs.

703 3.3.1. *The Precursory Cooling, the 2<sup>nd</sup> PCT and the Temperature Turnaround*

704 Attention is focused to nuclear fuel rod cooling after the occurrence of CHF and blowdown  
705 temperature rise depending upon heat stored in UO<sub>2</sub> pellets and LHGR. Film boiling and radiation  
706 heat transfer are concerned. Precursory cooling occurs prior to the arrival of the rewetting front and  
707 is due to entrained droplets originated by continuous flashing and possibly by accumulator injected  
708 liquid or, later on and with the same modalities, by LPIS actuation, [Svanholm et al., 1995](#), and  
709 [Chatzikyriakou et al., 2010](#). The entrained droplet may evaporate into the steam and act as a heat  
710 sink or may directly cool the clad by impinging. The last authors estimate that the heat extracted by  
711 those droplets directly impinging rods to be “*about 1/10 of the heat extracted by single-phase vapor under*  
712 *typical reflood conditions*”.

713 Precursory cooling, i.e. a film boiling heat transfer regime, causes a reduction in the slope of rod  
714 surface temperature rise or even a negative slope for the same quantity following the 2<sup>nd</sup> PCT; in the  
715 last case, the rod surface temperature turnaround occurs and local thermal-hydraulic parameter  
716 values are suited for rewet or Return to Nucleate Boiling (RNB) are discussed in section 3.4.

717 3.3.2. *The H<sub>2</sub> Production*

718 The production of H<sub>2</sub> constitutes a well-known and widely studied phenomenon associated  
719 with rod surface temperature excursion, e.g. [Shiozawa et al., 1982](#), see also the fundamental work by  
720 [Urbanic & Heidrick, 1978](#). The impact of the chemical reaction upon the LBLOCA evolution, which  
721 also implies addition of thermal energy into the system, becomes more and more important when  
722 clad temperatures overpass 600-800 °C. Acceptability thresholds in ECCS design, [USAEC, 1971](#), and  
723 countermeasures in containment, [OECD/NEA/CSNI, 1999](#), are established to deal with H<sub>2</sub>  
724 production.

725 As in previous cases, e.g. TPCF and CHF), it is well beyond the framework for the present paper  
726 to provide an outline of H<sub>2</sub> production and LOCA related effects.

727 The interaction between H<sub>2</sub> production, heat transfer coefficient including radiation and nuclear fuel  
728 performance (presence of crud and oxide, ballooning and burst, clad hydrating, etc.) during a  
729 transient (e.g. LBLOCA) needs more investigation.

730 3.4. *The Reflood and other Thermal-Hydraulic Phenomena*

731 The injection of borated water by Low Pressure Injection System (LPIS) starts when primary  
732 loop pressure reaches around 2 MPa. Massive amounts of coolant become available for core cooling,  
733 break flow decreases because of the low pressure difference between primary loop and containment  
734 and conditions for cooling of the core in forced circulation or nuclear boiling regimes are restored.  
735 Typically, the reflood process occurs during this period including quench front progression till the  
736 top of active fuel (actually two quench fronts are generated, see below; during the same period the  
737 equalization of pressures between primary loop and containment is established, thus terminating  
738 the blowdown.

739 3.4.1. *Quench Front Progression*

740 LPIS capability to quench the core after unavoidable dry-out occurrence during LBLOCA must  
741 be demonstrated, although reflood conditions may occur early during the transient depending upon  
742 the concerned reactor unit and the hypotheses adopted for the accident scenario. Recalling the  
743 following nomenclature to depict reflood may be of some interest: overpassing of Quench Front (QF)  
744 at a given axial location implies the occurrence of rewet and the Return to Nucleate Boiling (RNB)  
745 for that location; the temperature at the assigned location before the arrival of the QF may

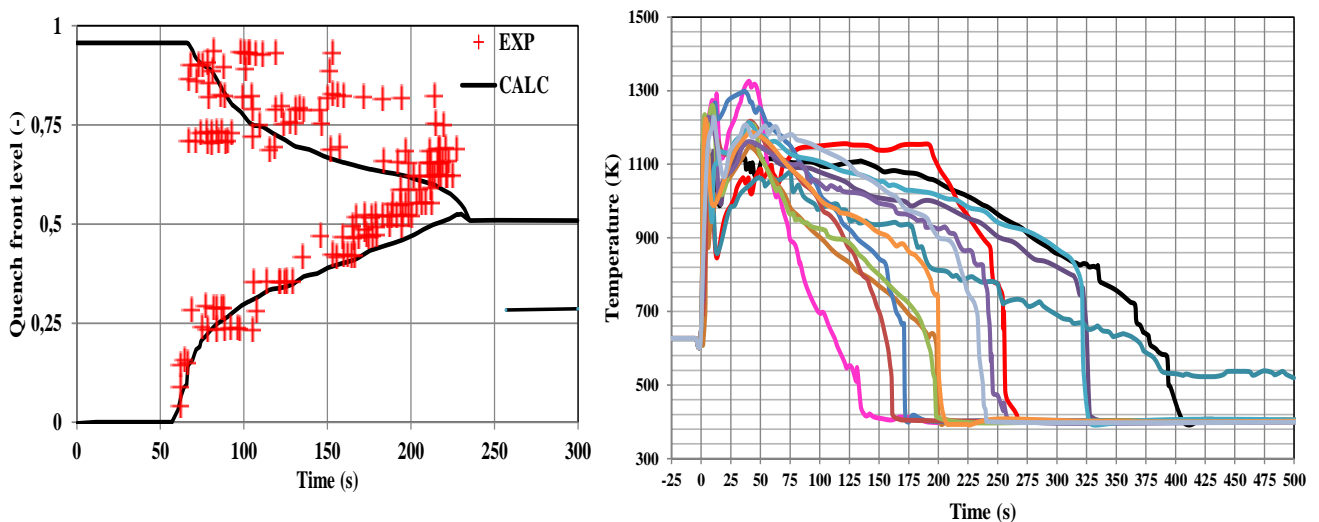
746 correspond to the Minimum Film Boiling (MFB). A picture of reflood phenomenology and related  
747 predictive capabilities can be derived from Fig. 11, Valette et al., 2011, and Reventos et al., 2008.

748 The phenomenology of QF progression in a typical PWR equipped with U-tubes steam  
749 generators, without hot leg injection, can be deduced from the left diagram in Fig. 11; the following  
750 notes apply:

- 751
- 752 • Bottom-up progression of the QF results from the bottom rising line: this is consistent with  
753 the increasing core collapsed level consequent to the LPIS injection in downcomer and prior  
754 refill of the lower plenum.
- 755 • Simultaneous occurrence of top-down QF progression occurs (top-down descending line):  
756 this is due to liquid transportation from the bottom-up QF in the form of droplets or even  
757 liquid slugs (in this case underlying the occurrence of Inverted Annular Film Boiling – IAFB  
758 – heat transfer and fluid flow regime).

759 The experimental data (red crosses in the diagram at about 220 seconds) show simultaneous  
760 reflood occurrence which is not predicted by the calculation: similar phenomenon was also detected  
761 by Svanholm et al., 1995, from the analysis of experimental data in Halden reactor.

762



763 **Figure 11.** Quench front progression (left, Valette et al., 2011) and reflood predictive capabilities  
764 (right, Reventos et al., 2008: application of different codes to LBLOCA analysis in PWR).

765 The right diagram shows the spread of data calculated by various codes for LBLOCA reflood:  
766 each line corresponds to a different calculation made by different code users; Zion (virtual or never  
767 operated) PWR unit is concerned. PCT (namely what has been called blowdown PCT) is calculated  
768 with a reasonable agreement by various code users; however, precursory cooling conditions for  
769 rewet and time of rewet occurrence show large discrepancies among the various calculations.

### 770 3.4.2. Other Thermal-Hydraulic Phenomena

771 Thermal-hydraulic phenomena in addition to those discussed in the present paper are relevant  
772 in case of LBLOCA in PWR (and PHWR) during each of the considered periods, as discussed by  
773 Aksan, 2017, D'Auria & Galassi 2017, and Aksan et al., 2018. A more comprehensive list of  
774 phenomena includes: ECCS bypass, steam binding, CCFL in different locations, pressure drop at  
775 geometric discontinuities, broken MCP fluid-dynamic resistance with free or locked rotor, two phase  
776 MCP (broken and intact loops) performance, condensation at ECC port, downcomer liquid  
777 penetration, mixing in different locations of primary loop, containment thermal-hydraulics. Those  
778 phenomena are indirectly embedded into the issues discussed in the paper and related predictive  
779 capabilities shall be associated with any computational tool (or numerical code) adopted for  
780 performing LOCA analyses.

781 3.4.3. The Fuel Behavior

782 The nuclear fuel constitutes the main target and motivation for the analysis of  
783 thermal-hydraulic phenomena during LBLOCA: a dynamic interaction happens between the fuel  
784 pins and the coolant. This is relevant during each identified period. After reflood no further  
785 mechanisms for fuel damage are expected: therefore nuclear fuel performance during LBLOCA is  
786 depicted hereafter by considering a list of physical processes causing degradation or rupture of fuel  
787 pins, namely occurring at high temperature and low coolant pressure:

- 788
- 789 • H<sub>2</sub> production following the Zircaloy-water chemical reaction discussed in section 3.3.
  - 790 • Ballooning of a few or of several rods, [Ammirabile & Walker, 2014](#): this causes obstruction  
791 to the coolant channels and interacts with QF progression.
  - 792 • Burst (following ballooning) and fission gas release, [Pontillon et al., 2001](#): the burst,  
793 following fuel fragmentation and relocation (see below) may cause release of long lived  
794 solid fission products into the coolant in addition to non-condensable gases.
  - 795 • Fuel relocation, [Kim et al., 2017](#), into the ballooned region which causes increase in local  
796 decay power production. This is preceded, depending upon burn-up, by fuel fragmentation  
797 (or even pulverization), [Brankov, 2017](#), see also [Bianco et al., 2015](#).

798 During the last two decades experimental research brought to better understanding of nuclear  
799 fuel weaknesses following in-core operation: high burnup is mainly concerned although  
800 “...fragmentation appears to almost always occur, regardless of burnup ...” (reference is made here to the  
801 current US licensing limit of 62 MWd/Ton U), [Raynaud, 2012](#). The weaknesses can be classified into  
802 three broad categories, synthesized by [D’Auria et al., 2019](#): (a) Pellet Clad Mechanical and Chemical  
803 Interaction (PCMI and PCCI), noticeably involving fuel swelling and cracking associated with core  
804 power ramps and reactivity excursions, e.g. [Sartoris et al., 2010](#); (b) clad-coolant chemical interaction,  
805 e.g. including oxide formation, appearance of hydride precipitates and occurrence of spalling and  
806 hydride rims, e.g. [Kim, 2011](#), (c) crud (or deposit) formation upon the clad, e.g. [Leyse, 2007](#). The  
807 nuclear fuel weaknesses interact with the listed degradation mechanisms in case of LOCA (bullet  
808 item above) creating complex fuel failure conditions; see e.g. [Rozzia et al., 2012](#): expected fuel  
809 failures oriented USNRC to propose modification in acceptance criteria, [USNRC, 2018](#).

810 3.5. The Long Term Cooling – the Sump Recirculation

811 Once the core is covered by borated liquid water at a temperature below the saturation value,  
812 the pressure in primary loop and in containment is the same and the LPIS is in operation according  
813 to design, steady state conditions are reached and the transient (LOCA) period is concluded.  
814 However, fission product decay is still producing thermal power in the order of 1% of  
815 initial-nominal reactor power (or about 40 MWth in a 1000 Mwe NPP unit) and LPIS tanks are going  
816 to be emptied in some minutes: safe conditions must be ensured during some time without the  
817 support of energy sources or human actions outside the NPP site (typically, 8 and 72 hours, for  
818 existing and new reactors, respectively). Those conditions are achieved by so called containment  
819 sump recirculation: the sump at the bottom of containment is filled with steam water mixture  
820 coming from the break and condensed into the containment and LPIS pumps suction is switched  
821 from the tanks to the sump. The safety and design issues of concern are:

- 822
- 823 • Liquid level and temperature in the sump should be consistent with pump Net Positive  
824 Suction Head (NPSH).
  - 825 • Debris formed during LOCA, namely around the break location should not induce pump  
826 cavitation, or, in the case of ‘small debris’, should not accumulate in narrow passages as in  
827 the core inlet.

828 Addressing the first item implies performing coupled primary system / containment analyses,  
829 e.g. [Mascari et al., 2012](#). A technological challenge is connected with the latter item; e.g. [Lee et al.,  
830 2014](#), and [Azam et al., 2018](#).

831 3.6. *Licensing, V&V, Scaling and Uncertainty*

832 The phenomenological picture provided for LBLOCA shall be integrated into the licensing  
833 process. The application of numerical codes is needed in order to fulfill licensing related regulatory  
834 requirements; namely, those codes can be considered as the bridge between individual reactor  
835 features, phenomena and requirements.

836 A suitable description of licensing framework, code development and code application  
837 procedures may require textbooks and is well beyond the present framework. Hereafter, a synthesis  
838 discussion is provided in relation to:

- 839 a) The connection between LBLOCA phenomenology (or physical aspects) and the licensing  
840 requirements.
- 841 b) The key elements which constitute the Best Estimate Plus Uncertainty (BEPU) approach for  
842 code application into the licensing process.

843 3.6.1. Cross-Link between Physical Aspects of LBLOCA and Licensing Needs

844 ECCS licensing targets, can be found in [USAEC, 1971](#); details needed for demonstrating the  
845 acceptability of analyses can be found in [USNRC, 2013](#), (NUREG-0800, continuously updated).

846 Selected licensing needs are summarized in Table 2 (heading) and cross-linked with the  
847 LBLOCA physical aspects identified in sections 3.1 to 3.6 [lines 1 to 20; the words ‘physical aspects’  
848 are used to distinguish from ‘phenomena’ used by [Aksan et al., 2018](#)]. It can be noticed that: (1) each  
849 of the needs is considered by at least one physical aspect; (2) each concerned LBLOCA aspect  
850 addresses at least one licensing need; (3) other phenomena (list in section 3.4) line 20, are all relevant  
851 in LBLOCA analyses and, without providing details, are assumed contributing to the demonstration  
852 of accomplishment of each identified need.

853 3.6.2. Key Elements of BEPU

854 The simplest definition tells that BEPU is an approach for the application of Best Estimate (BE)  
855 codes and related (or ‘Plus’) Uncertainty (PU) to the licensing process for the evaluation of reactor  
856 safety, [D’Auria, 2018](#). Other than a code and an uncertainty method, six characterizing elements for  
857 BEPU have been identified:

- 858 1) The phenomena.
- 859 2) The V&V (Verification and Validation).
- 860 3) The scaling.
- 861 4) The code coupling.
- 862 5) The framework and the requirements for AA part of the Final Safety Analysis  
863 Report (FSAR).
- 864 6) The qualification of the code users or analysts.

865 Phenomena, item 1), have been discussed in sections 3.1 to 3.5 and regulatory framework, item  
866 5) has been mentioned in previous paragraph. The Verification and Validation (V&V), item 2), is  
867 expected to be a part of BEPU because of unavoidable approximations embedded into the  
868 development of a code, e.g. see [D’Auria & Lanfredini, 2018](#), for new perspectives in the area. Scaling  
869 analysis, item 3), is essential because most of data for validation are available for parameter ranges  
870 different from those applicable to reactors, [OECD/NEA/CSNI, 2017](#). Different numerical codes need  
871 to be coupled, item 4), in order to perform a BEPU application, [IAEA, 2007](#): the demonstration of  
872 qualification of coupling constitutes the concern here (and shall be part of BEPU). Finally, the  
873 qualification of analysts in charge of BEPU application, item 6), needs proper consideration, e.g.  
874 [Ashley et al., 1998](#). BEPU description is completed by a few dozen additional ‘framework elements’,  
875 as discussed by [D’Auria, 2018](#).

876  
877  
878  
879  
880

Table 3. Cross-link between selected LBLOCA phenomena and licensing needs.

N	[Licensing requirement] →	ECCS design – PCT	ECCS design – 17% ECR	ECCS design – H <sub>2</sub>	Core integrity (ECCS design)	ECCS design – long term cooling	Nuclear fuel integrity	Containment integrity	Notes
	[LBLOCA physical aspect] ↓								
1	Break Opening Time (BOT)				X*				* Core integrity not affected by ECCS design.
2	Depressurization wave				X*				
3	Jet impingement & Thrust							X	
4	Pipe Whip & Missiles							X	
5	Loads on internals				X*				* see note at line1
6	Flashing	X							
7	Core flow reversal	X							
8	Fission Power Peak	X					X		Only in PHWR
9	Boron injection	X					X		
10	TPCF	X	X	X				X	
11	Flow stagnation	X							
12	CHF & blowdown, (1 <sup>st</sup> ) PCT	X							
13	Early core rewet		X	X					
14	Depressurization rate	X	X	X					
15	Containment pressure							X	
16	Precursory cooling, (2 <sup>nd</sup> PCT) and temperature turnaround	X	X	X					Conditions for reflood
17	H <sub>2</sub> production			X				X	
18	Quench progression & RNB		X	X					
19	Long term cooling					X		X	Sump recirculation & debris
20	'Other' phenomena	X	X	X	X	X	X	X	Listed in section 3.4

#### 882 4. The ATUCHA-II LBLOCA Safety Evaluation

883 In 2006, the Argentinean Government set the financial framework and requested the NA-SA  
884 Company to complete the construction of Atucha-II. About ten year before the Siemens (German  
885 Company) had delivered all main components of the nuclear reactor on the site and basically  
886 completed the technology transfer connected with the PHWR design. The same company was not  
887 any more available to resume the construction activities in 2006; then, NA-SA took the decision to  
888 bring the reactor in operation without the direct support of the original reactor designer. In this  
889 framework University of Pisa was asked to contribute to the Final Safety Analysis Report and,  
890 namely to issue the Chapter 15 dealing with accident analysis.

891 The activity was accomplished by GRNSPG of University of Pisa at the due time, involving a  
892 properly established international group of senior consultants. A suitable version of the FSAR was  
893 submitted to Argentinean Regulatory Body (ARN) in 2010 (and later on endorsed by the same Body)  
894 and the reactor was connected to the electrical grid for continuous operation in 2014.

##### 895 4.1. The Framework for the Activity

896 Starting from 2006, three main lines of activity were pursued at University of Pisa in relation to  
897 Atucha-II:

- 898 ➤ LBLOCA analysis and understanding of inherent design features, *D'Auria et al., 2008.*

- 899       ➤ Formulation of a BEPU approach (approved by Regulatory Body), [Muellner et al., 2008](#).  
900       ➤ Application of the BEPU approach for issuing the Chapter 15 of the FSAR, [GRNSPG, 2010](#).

901       It shall be noticed in advance that the understanding of the system design features and the  
902 confirmation of available safety margins was possible only with BEPU and utilizing techniques and  
903 research findings not available at the time of the design of the Atucha-II PHWR.

904       Hereafter, achievements from the LBLOCA analysis are outlined: reported data are not  
905 necessarily part of the licensing documentation, [GRNSPG, 2010](#); rather, results from safety  
906 evaluations and supporting studies for the FSAR are reported and discussed; the technological  
907 framework established in section 3 is considered to this aim.

908       The BEPU approach had a key role for the issuing of FSAR Chapter 15. However a number of  
909 related papers have been already published: reference to those papers is provided in section 4.4  
910 together with a list of performed key activities.

#### 911 4.2. Background analysis and challenges

912       Two statements summarize the start of Atucha-II LBLOCA activities at University of Pisa:

913       < [A] All design documents and information (noticeably including access to components and systems as built)  
914 from the technology transfer (i.e. from the original designer to the utility in Argentina) related to Atucha-II are  
915 available >.

916       < [B] A positive void reactivity coefficient is expected to produce a fission power excursion after LOCA: safety  
917 margins need to be (evaluated independently from designer and) confirmed >.

918       The former statement implied a few million pages documents possibly needed to understand  
919 the project details; the latter should be taken considering that in the aftermath of the power  
920 excursion in Chernobyl, (i.e. for 2 decades at the time of the start of activities) no reactor in the world  
921 was put in operation with a positive void coefficient. Therefore the Atucha-II project, or a  
922 stimulating endeavor, started.

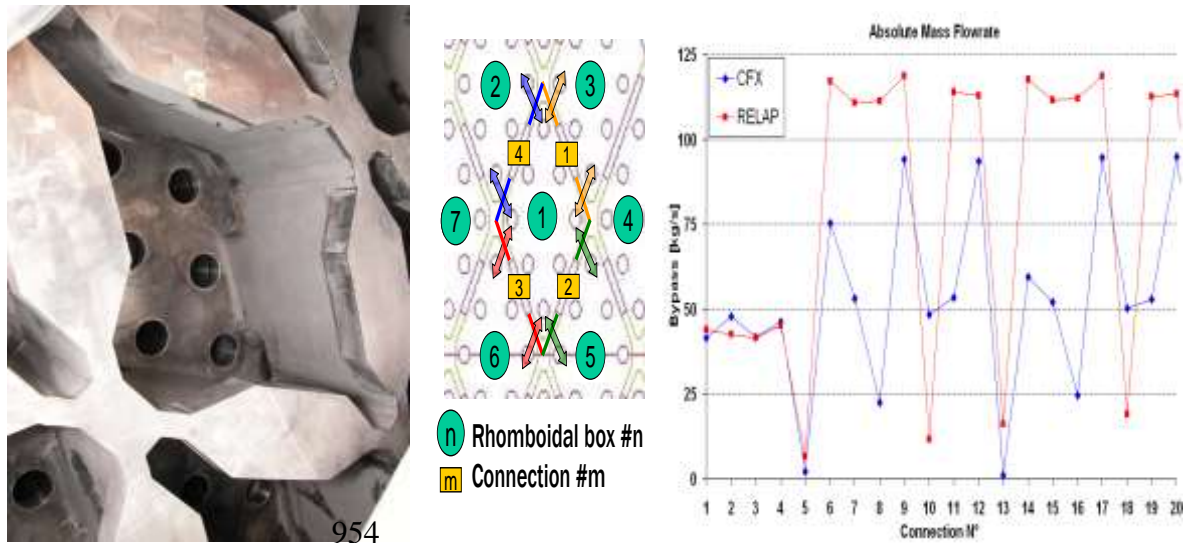
923       Two intrinsic challenges for the project are directly derived from the PHWR description (section  
924 2.1): the use of D<sub>2</sub>O as coolant/moderator and the features of the moderator system imposed  
925 preliminary investigation to confirm the applicability of adopted computational tools. Errors in  
926 experiments where operational fluid is H<sub>2</sub>O and D<sub>2</sub>O were compared (former challenge); modeling  
927 of a dozen RPV bypass flow paths was needed (latter challenge) to simulate two parallel loops, PS  
928 and moderator, at different temperatures and driven by separate pumps ending up at the same  
929 pressure into the RPV.

930       A list of ten additional (selected) challenges which needed to be considered prior to start of  
931 safety margins calculation is [note-1, adopted abbreviations are: BA = Break Area; BIT = Boron Injection  
932 Time; BOT = Break Opening Time; BP = Break Position (along the loop); CCFL = Counter Current Flow  
933 Limitation; CL = Col Leg; FA = Fuel Assembly; FPP = Fission Power Peak; G/P = Mass flowrate divided by  
934 power produced in each FA; HL = Hot Leg; LP = Lower Plenum; MCP = Main Coolant Pump; PCT = Peak  
935 Clad Temperature; RPV = Reactor Pressure Vessel; note 2: FPP may not coincide with Total Power Peak (TPP)  
936 where all contributions to core power are included, e.g. decay power]:

- 937       [1] LP modeling.
- 938       [2] PCT vs (BA and BP).
- 939       [3] FPP vs (BA and BP).
- 940       [4] FPP vs (BOT and BIT).
- 941       [5] (PCT and FPP) vs ECCS configuration.
- 942       [6] (PCT and FPP) vs core life.
- 943       [7] Initial void content, MCP operation and single failure.
- 944       [8] BA based on the as-built CL nozzle connection and RPV.
- 945       [9] CCFL in HL.
- 946       [10] G/P in each FA (nominal operation).

947       [1] The Atucha-II RPV-LP is filled by blocks of inert material in order to decrease the amount of  
948 expensive heavy water. The LP function to create a uniform upper oriented flow towards the core  
949 (case of PWR) is taken by a plate formed by rhomboidal boxes, sketch given in Fig. 12 (left and  
950 center): each box has vertical holes connecting with fuel channels and horizontal flow passages

951 (arrows in the center sketch) to uniform the pressure at core inlet. Results to demonstrate  
 952 applicability of a system code are given in the right sketch compared with CFD code results.  
 953



955  
 956 **Figure 12.** Left: view from the bottom of one rhomboidal box core support plate. Center:  
 957 identification of box and of horizontal 'bypass' paths; Right: detail of qualification results for the  
 958 system code model.

959 [2] Break area and position affect PCT in Atucha-II in a similar way as in PWR, as shown  
 960 (sample results) in left side of Figs. 4 and 5, respectively. The difference is that, in the current  
 961 situation, the FPP has also an impact upon PCT (further discussion below).

962 [3] FPP expected in case of PHWR LBLOCA is affected by parameters different from those  
 963 influencing PCT: a specific sensitivity study was needed with sample results shown in right sides of  
 964 Figs. 4 and 5, respectively related to BA and BP dependencies.

965 [4] BOT has negligible impact on PCT in case of PWR where fission power shifts to decay power  
 966 immediately after the break occurrence; this is not the case of PHWR where void formations in the  
 967 core, affected by BOT, determine a FPP. Therefore, the Fast Boron Injection System was added to the  
 968 Atucha-II design: the actuation of the system is characterized by the BIT parameter. BIT is defined as  
 969 the time when the first droplet of highly borated liquid reaches the moderator: at that moment the  
 970 'same droplet' had already interacted with the intrinsic neutron reflector at core top affecting fission  
 971 power generation.

972 Selected results obtained by a simplified nodalization (nodalization discussion in section 4.4.2)  
 973 are summarized in Fig. 13.

974 The support analyses (not necessarily characterized by reported data) demonstrated that:

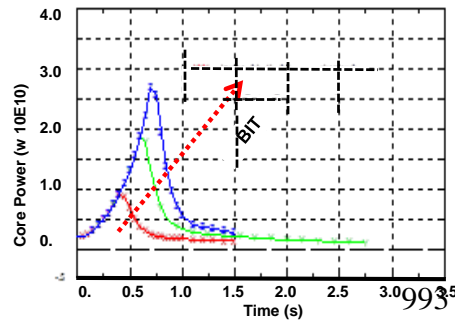
- 975 • BOT values  $\geq 1$  s suppress any FPP.
- 976 • BIT values  $\leq 0.3$  s suppress any FPP; otherwise BIT values  $\geq 1.0$  s are ineffective in reducing  
 977 FPP.
- 978 • The largest values for PCT and FPP are obtained for a BA (slightly) lower than the maximum  
 979 attainable area (i.e. the DEGB of the CL): early and increased core flow reversal (and  
 980 connected core cooling) contributes to this outcome (see also Figs 4 and 5).

981 The importance of BIT suggested the construction of a 'scale 1' test facility, called BITF (= Boron  
 982 Injection Test Facility), [Moretti et al., 2018](#): performed experiments brought to an improvement of  
 983 the system and confirmed the design parameters adopted in licensing analyses.

984 [5] The lack of symmetry of the Atucha-II system, the availability of four trains (each one having  
 985 50% capability of core cooling) per ECCS (noticeably accumulator and LPIS) and the licensing need  
 986 to exclude the most effective train brought to a complex analysis. The worst conditions for the  
 987 LBLOCA had to be identified by combining the selected ECCS configuration with BA and BP.  
 988



989  
990  
991  
992



Injection (sec)	45kw/m Break PCT					
	0	0.1	0.3	0.5	0.7	1
0.1	1	11	21	31	41	51
0.2	2	12	22	32	42	52
0.3	3	13	23	33	43	53
0.4	4	14	24	34	44	54
0.5	5	15	25	35	45	55
0.6	6	16	26	36	46	56
1	10	20	30	40	50	60

	<1200
	>1200
	>1300
	>1400
	>1500
	>1600

Injection (sec)	45kw/m Break Energy to the fuel					
	0	0.1	0.3	0.5	0.7	1
0.1	1*	11*	21*	31*	41	51
0.2	2	12	22	32	42	52*
0.3	3	13	23	33	43	53
0.4	4	14	24	34	44	54
0.5	5	15	25	35	45	55
0.6	6	16	26	36	46	56
1	10	20	30	40	50	60

	<840
	>840
	>840

994  
995

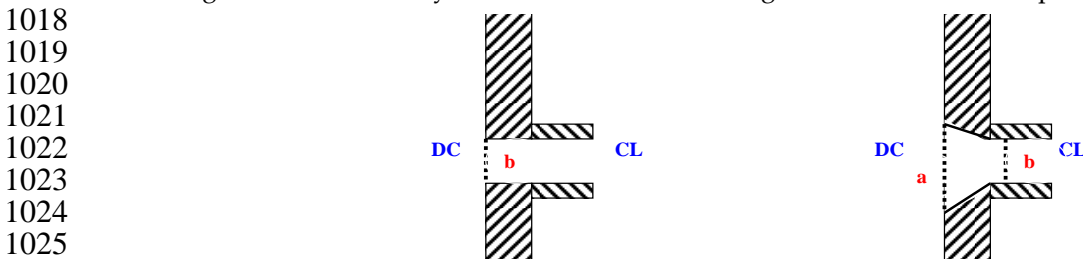
996 **Figure 13.** Top: FPP calculated for different BIT (0.4, 0.6 and 0.7 s from bottom to top). Bottom:  
997 relationship between BIT, BOT, PCT [°C] and FPP (energy to the fuel, [Cal/g]) at LHGR limit value.

998 [6] Daily changes of fuel characterize the operation of natural uranium PHWR; this implies  
999 change in core power distribution, average burn-up and, consequently, fuel material properties  
1000 during the core life. Noticeably, maximum LHGR and void coefficient change during the core life. A  
1001 specific core-life analysis led to identify an equilibrium cycle the worst LBLOCA conditions.

1002 [7] Several “settings”, other than those already discussed, have to be justified for a suitable  
1003 LBLOCA licensing analysis, like initial pressurizer level, steam generator pressure and initial core  
1004 power. Assumptions for (a) fluid sub-cooling and sub-cooled void content in individual channels at  
1005 the time of the LBLOCA start, (b) the operation of MCP, and (c) the worst single failure in active  
1006 components, in addition to the failure of one ECCS train, constituted examples of formidable targets  
1007 for investigations which had to be completed prior to the start of an acceptable licensing study. In  
1008 relation to the item (a), for an equilibrium core condition, the following was found:

- 1009 • Fluid temperature sub-cooling at core outlet in the range (0 – 25) K and average value of 10 K;
- 1010 • Sub-cooled voids are present (void fraction up to 0.4) at the outlet in (10 – 20)% of core channels;
- 1011 • High average void contents at LBLOCA start may imply lower contribution of voids to FPP.

1012 [8] The reference geometric configuration for the connection region between the RPV and the  
1013 CL is shown in the left sketch of Fig. 14, together with the actual (as built) configuration in Atucha-II.  
1014 Let’s consider:  $G_{c^{ref}}$  = (initial value of) critical flow-rate adopted in final (licensing) analysis  
1015 consistent with the left sketch;  $G_{c^{cathare}}$  = (initial value of) critical flow-rate derived from modeling the  
1016 sketch on the right by Cathare code;  $G_{gas^{cfd-left}}$  and  $G_{gas^{cfd-right}}$  = left and right values of (stationary)  
1017 critical gas flow obtained by CFD calculations assuming an infinite reservoir upstream the break.



1026 **Figure 14.** Sketch for CL to RPV connecting nozzle. Left: typical PWR. Right: Atucha-II PHWR.

1027 Starting from the ratio  $a/b = 1.52$  (Fig. 14), the following results were obtained:  
1028

$$(G_{c,cathare} / G_{c,ref}) = 1.5 \quad \text{and} \quad (G_{gas,cfd-right} / G_{gas,cfd-left}) \leq 1.15$$

Flowrate values related to the right sketch in Fig. 14 were not considered in final (licensing) analyses because (a) they bring to reduction in PCT and FPP (see Fig. 4); (b) lack of experimental data prevented the possibility to demonstrate a suitable qualification for the obtained results.

[9] The capability to predict delivery into the upper plenum of the ECCS liquid injected in HL (related phenomenon called CCFL in HL) is difficult due to the momentum of ECC water directed towards the upper plenum [Damerell & Simons (Eds.), 1993]. CCFL in hot leg under reflux condenser conditions is described by Glaeser & Karwat, 1993, for example. This implies

$$(Jg^*)^{0.5} \approx 0.7,$$

where  $Jg^*$  is the non-dimensional value of vapor superficial velocity at the concerned (HL nozzle in this case) CCFL location. Recent available documents (i.e. published after the completion of Atucha-II licensing) confirm the above statement; see e.g. Fig. 15, Deendarlianto et al., 2012, where data predicted by Chun & Yu, 2000, are reported too (Chun & Yu data are obtained by an empirical correlation qualified by an experimental data-set measured in a pipe with a diameter about 10 times smaller than the HL of Atucha-II).

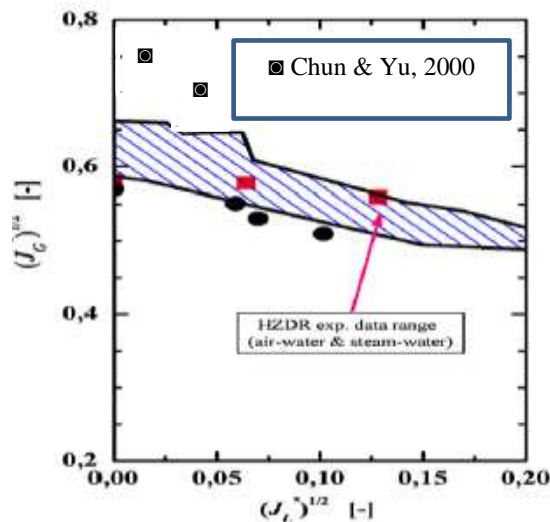


Figure 15. CCFL data relevant to the Atucha-II LBLOCA at the HL-RPV connection.

The status of knowledge for CCFL (namely at the HL-RPV connection) after the completion of the Atucha-II licensing can be summarized, according to Deendarlianto et al., 2012, as “... presently we have no physical measure to capture the important parameters of CCFL. ..., if we change the test liquid temperature, the physical properties of the liquid also change which accordingly affects the interfacial heat transfer between gas and liquid.” Insights about the steps undertaken to optimize the CCFL modelling capabilities for the Atucha-II application are provided in section 4.4.2

[10] The ratio mass flowrate / power generated (G/P) in each FA is given in Fig. 16. In a typical operational condition this ratio has a complex distribution and numerical values across the core in the range 4 to 7 (concerned units) can be noted. Selected key aspects of LBLOCA which are affected are:

- Early void generation is different in different FA.
- Flow reversal occurrence is expected at different times.
- Energy stored in fuel pins is affected in addition to LHGR (different fluid temperature at pin surface)
- FPP is expected at different times.
- PCT in individual FA is largely affected by G/P because of all of above.

1082  
 1083  
 1084  
 1085  
 1086  
 1087  
 1088  
 1089  
 1090  
 1091  
 1092  
 1093  
 1094  
 1095  
 1096  
 1097

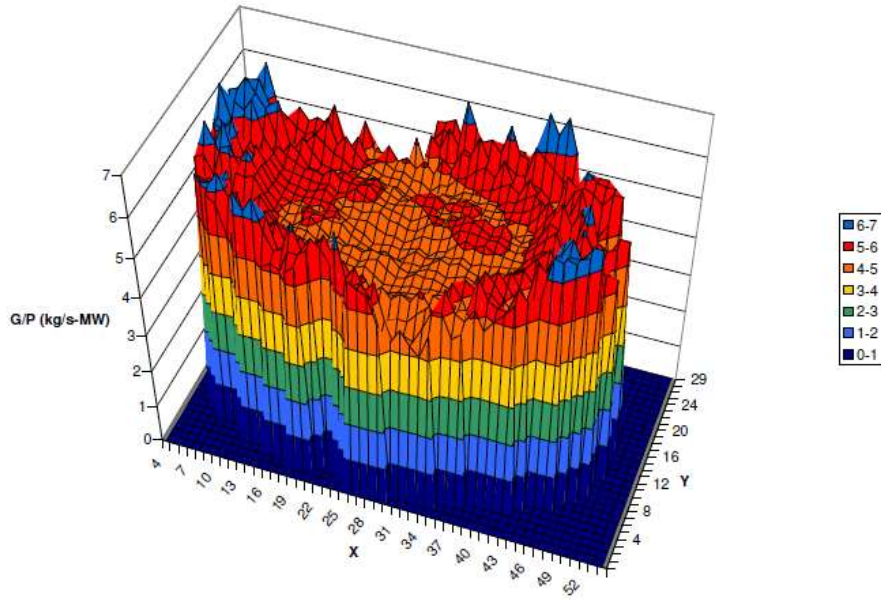


Figure 16. G/P ratio in each FA of Atucha-II core.

1098 4.3. The key results

1099 LBLOCA calculations for Atucha-II were performed based on the available background  
 1100 information (chapter 3) with main attention for challenges (selected ones in section 4.2). A  
 1101 qualitative and quantitative picture of results can be drawn from Fig. 17 and Table 4, respectively.

1102 The reported values, as indicated in the note under the 4<sup>th</sup> column in Table 4, do not coincide  
 1103 with the proprietary licensing data. Rather, those values relate to safety supporting calculations and  
 1104 provide a 'meaningful' picture of the transient scenario.

1105  
 1106  
 1107  
 1108  
 1109  
 1110  
 1111  
 1112  
 1113  
 1114  
 1115  
 1116  
 1117  
 1118  
 1119

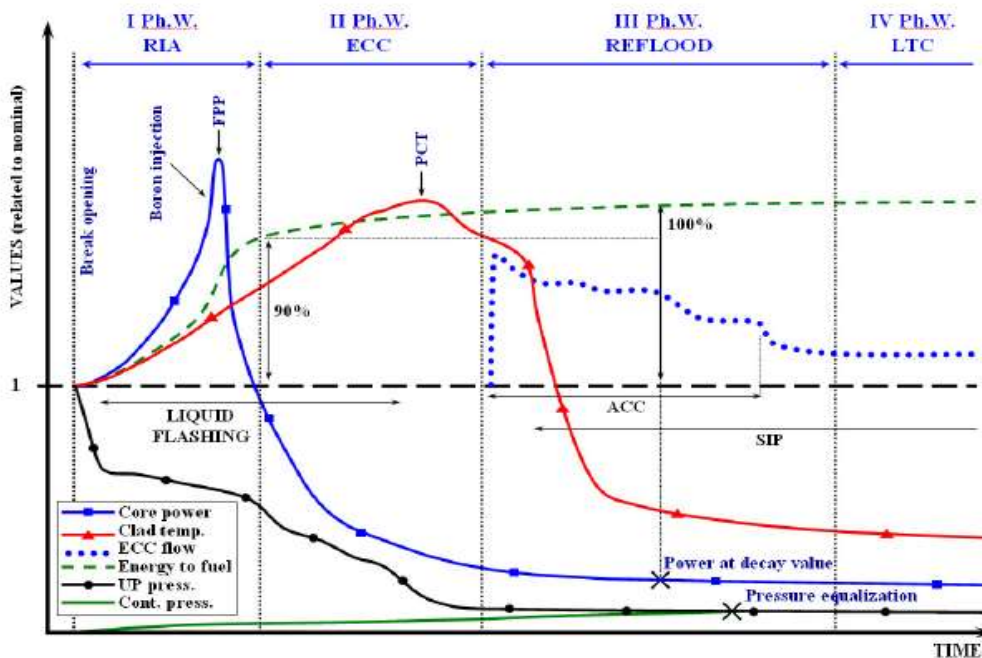


Figure 17. A picture of the LBLOCA scenario predicted for Atucha-II.

1121

**Table 4.** An overview of Atucha-II LBLOCA: sequence of events and phenomena.

N	Phenomenon, Event or LBLOCA Aspect	Unit	Value		Notes
			Licensing	Safety	
1	Break occurrence	s		0.	
2	BOT	m-s		1. – 30.	Sensitivity studies (sect. 4.1)
3	Load on RPV support	Ton		< 1500	No or limited (acceptable) damage to containment structures and to RPV support
4	Jet impingement load	Ton		< 1100	
5	Reactor cavity pressurization	MPa		0.8	
6	Stress on moderator tank	MPa		< 430	ASME criteria fulfilled
7	BIT	s		0.6	
8	FPP	Mwth		21.	at $\approx 0.6$ s ; $\approx 50$ Cal/g energy
9	Decay power reached	s		15.	After FPP
10	Void appearance in the core	s		0.01 – 1.0	Depending upon location
11	Flow reversal at core inlet	s		0.05 - 0.1	Not occurring in each channel
12	Flashing in upper plenum	s		2.	Bulk values connecting pressure decrease and initial temperature (range in the case of moderator)
13	Flashing in downcomer / LP	s		13.	
14	Flashing in moderator	s		35. – 80.	
15	CHF	s		0.5 – 1.	Not occurring in each channel
16	PCT	K		< 1350	At about 5 s; including uncertainty
17	Containment pressure peak	MPa		0.35	At about 10 s
18	PRZ emptied	s		28.	Pressure equalization with PS
19	Minimum RPV mass inventory	%		20.	Excluding the moderator
20	Accumulator injection start	s		15.	
21	Accumulator emptied	s		150. – 170.	
22	LPIS injection start	s		100.	SIP in Fig. 17
23	Reflood completed	S		200.	
24	Collapsed level above core	S		240.	
25	Equal p in containment and PS	S		250.	Pressure equalization
26	Sump recirculation start	S		800.	Time of emptying of LPIS tanks
27	Sump level and temperature	m/°C		> 1 / < 80	At above time
28	Fraction release of (Xe&Kr)/(I)	-		1. / < 0.4	
29	Radiation impact	Sv		< 0.1	Event duration in LPZ
30	End of calculated transient	S		1000.	

Reported values (column on the right) do not coincide with licensing values (because of proprietary data). Reported data allow capturing the relevant LBLOCA phenomenology.

1123

1124

Explanatory notes for Fig. 17 and Table 4 are (additional insights can be found in sections 4.3.1 to 4.3.5):

1125

1126

❖ Four phenomenological windows (PHW) are established and are characterized by (1<sup>st</sup> PHW) the FPP occurrence, (2<sup>nd</sup> PHW) the PCT occurrence, (3<sup>rd</sup> PHW) the actuation of ECCS and the reflood, (4<sup>th</sup> PHW) the long term cooling and the sump recirculation.

1127

1128

❖ No argument could be used to justify (for regulators), or to substantiate (from a technology viewpoint), a BOT value greater than 1 m-s (line 2 in Table 4): this value was conservatively assumed in the licensing analysis.

1129

1130

❖ Flashing occurs during the 1<sup>st</sup> PHW up to the 3<sup>rd</sup> PHW: however early flashing consequence of pressure wave propagation should be distinguished from depressurization originated flashing.

1131

1132

❖ The loads generated by two-phase jet are considered in lines 3 to 5 (Table 4); pipe whip was evaluated as uninfluential because of design countermeasures.

1133

1134

❖ Noticeably, sump level formation and presence of debris are considered during the 4<sup>th</sup> PHW.

1135

1136

1137

1138

1139

A typical PWR LBLOCA scenario (PRZ, PS and containment pressure, CHF and flow reversal occurrence, rod surface temperature excursion, ECCS actuation and reflood) constitutes the outcome for the Atucha-II PHWR prediction. Key difference related to a PWR is the occurrence of the FPP and the need for fast boron injection: the FPP has an impact over PCT and the integrity of fuel which needed specific investigation. Emphasis is given in sections 4.3.1 to 4.3.5 to peculiar aspects of

1140

1141

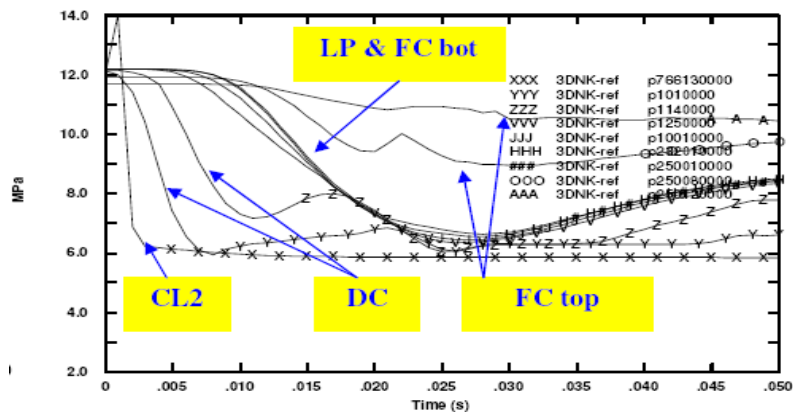
1142

1143 Atucha-II PHWR LBLOCA; description of established LBLOCA parameters (depressurization rate,  
1144 reflood phenomenology, etc.) is omitted.

#### 1145 4.3.1. The BOT and the Loads Generated by Pressure Wave Propagation (PHW 1)

1146 A specific activity was carried out for Atucha-II in order to demonstrate a BOT > 1 s for DEGB  
1147 LBLOCA: this would imply a negligible FPP, as already mentioned. To this aim, Zhang et al., 2013,  
1148 started their work considering that Stress Corrosion Cracking (SCC) is an issue with many PWR  
1149 plants; therefore, an upper bound SCC growth curve was used to envelope both Primary Water  
1150 Stress Corrosion cracking (PWSCC) and intergranular stress corrosion cracking (IGSCC). The pipe  
1151 material in Atucha-II is 20MnMoNi55 (similar to A533B) and at this time is not known to be  
1152 susceptible to SCC; nevertheless, a high crack growth rate was used so that after 80 years of  
1153 operation the concerned degradation may occur. This consists of a circumferential through wall  
1154 crack of 120 °; then a hypothetical earthquake was assumed having maximum amplitude of the  
1155 acceleration wave much higher than the design earthquake. In such a situation it is impossible not to  
1156 realize that there was a leak, or the LBB concept could be adopted to prevent LBLOCA; furthermore,  
1157 even in the absence of leak detection (or LBB not 'working'), a through wall crack ended into a 2A  
1158 break in a couple of seconds. This result was used within licensing process; otherwise information  
1159 below relates to BOT ≈ 1 m-s.

1160 The (negative) pressure wave propagation from the break towards the RPV can be observed in  
1161 Fig. 18. The lowest pressure, detected soon after the break occurrence in the CL, has a value below  
1162 the local saturation value corresponding to the initial temperature (similar situation observed in  
1163 HDR experiment, Fig. 7). The amplitude decreases when the pressure wave moves from CL to  
1164 downcomer and to lower plenum; with an approximate delay of 20 m-s the wave reaches the bottom  
1165 of the fuel channels and propagates upwards where about one-half amplitude can be seen. Not  
1166 shown in the diagram, the moderator pressure remains at the initial value during the reported time  
1167 span (horizontal axis in Fig. 18).



1168

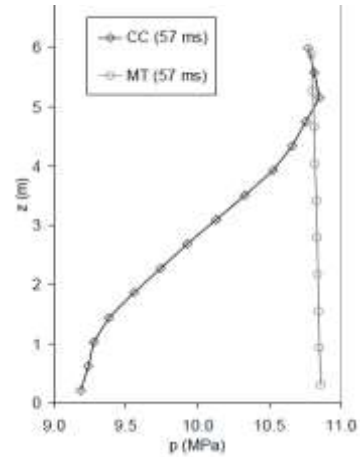
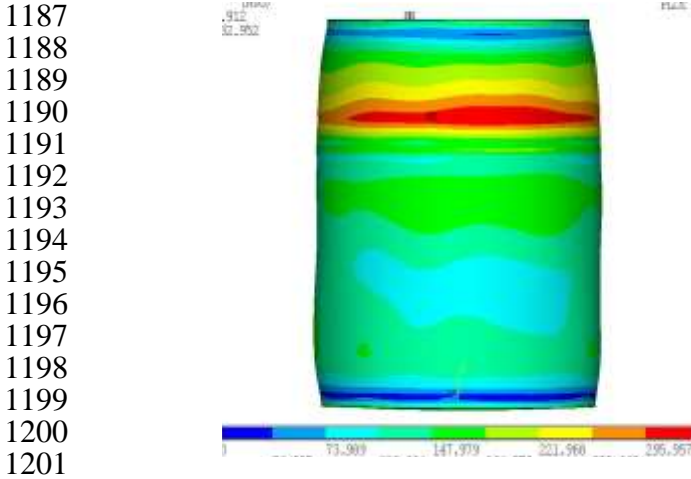
1169 **Figure 18.** Atucha-II LBLOCA: propagation of depressurization wave from the break.

1170 The wave propagation produces an impulse pressure load acting from the inside to the outside  
1171 in the case of the moderator tank, Fig. 19 left, and from outside to the inside of fuel channel walls,  
1172 Fig. 19 right. The location of the maximum stress value can be observed in Fig. 19 at the concerned  
1173 time.

#### 1174 4.3.2. Coupling between Thermal-Hydraulics and Neutron Physics (PHW 1)

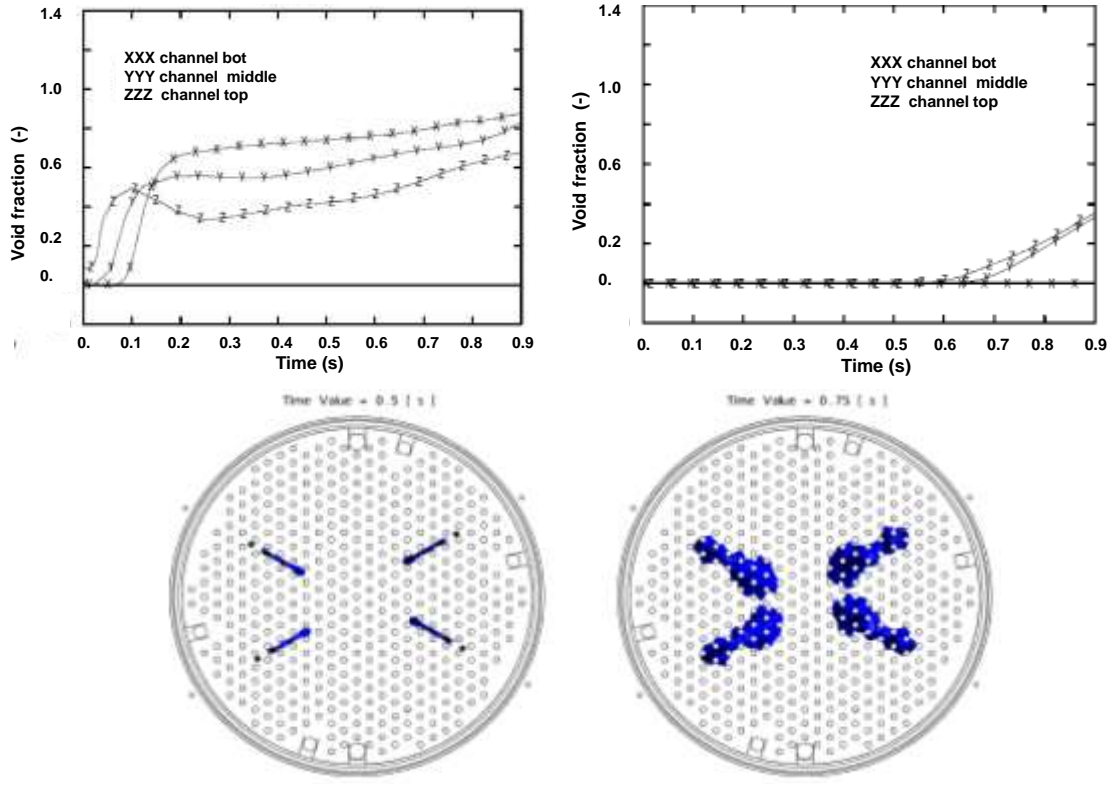
1175 The pressure wave propagation in the fuel channels generated early voids which depend upon:  
1176 a) location of channels in the core related to the CL where the break occurs: closer channels are  
1177 affected earlier;  
1178 b) channel orifice: the smaller the flow area at fuel channel inlet the smaller is the pressure  
1179 wave amplitude into the channel;

- 1180 c) distance from channel bottom: upstream pressure wave propagation (and void generation)
- 1181 is affected by distance from channel inlet and flow conditions (see also item below);
- 1182 d) fluid temperature profile in each channel: subcooling at channel inlet is the same in all
- 1183 channels, however, G/P ratios and total power are different in each channel (see also Fig. 16)
- 1184 and in some channels subcooled void is present at the top (see also challenges [7] and [10]
- 1185 under section 4.3): therefore each channel has, (1) a different feedback in terms of void
- 1186 production, and (2) a different impact upon local and global fission power.



1202 **Figure19.** Atucha-II LBLOCA at 0.05 s. Left: pictorial view of moderator tank load. Right: pressure  
 1203 difference across one selected fuel channel.

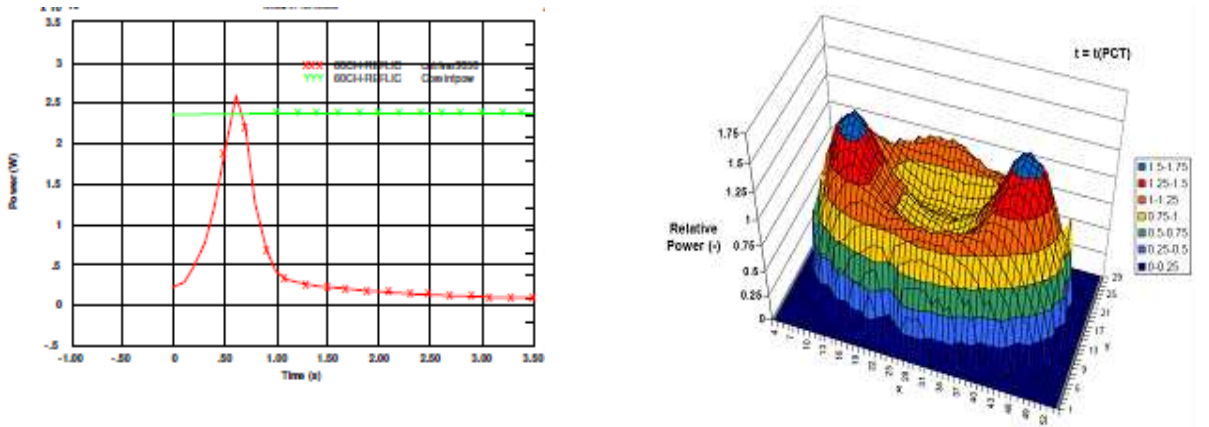
1204 Differences in terms of void generation between two typical channels and among (three  
 1205 selected) axial locations inside each individual channel can be drawn from top of Fig. 20.



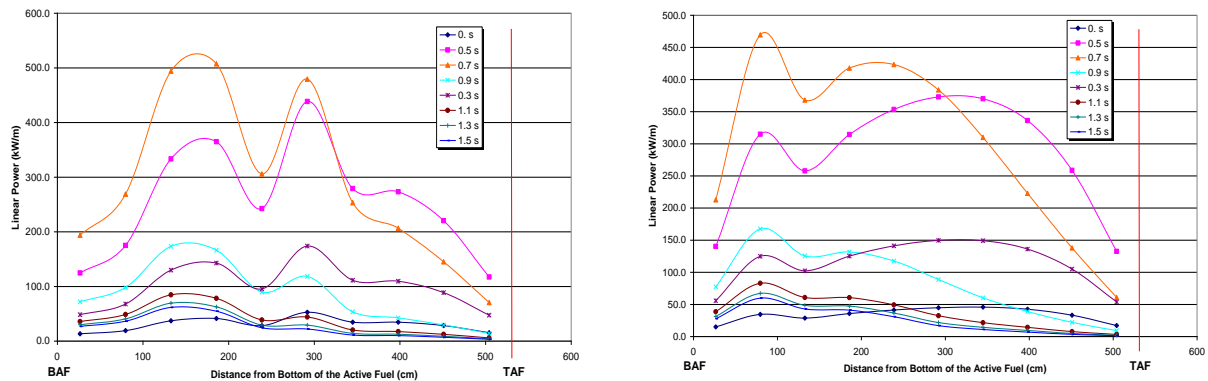
1206  
 1207  
 1208  
 1209  
 1210  
 1211  
 1212  
 1213  
 1214  
 1215  
 1216  
 1217  
 1218  
 1219 **Figure 20.** Atucha-II LBLOCA, bases for the evaluation of FPP. Top: void fraction in two different  
 1220 channels at three different elevations originated by propagation of depressurization wave from the  
 1221 break. Bottom: top view of boron cloud formation in the moderator tank.

1222 The end components of the Boron Injection System consist of four lances which penetrate the  
 1223 moderator tank, each one having several holes and an angle related to the axis of the tank. The  
 1224 arrival time of borated fluid into the moderator tank has been called BIT (see challenge [4] and line 7  
 1225 in Table 4). In addition to BIT, the diffusion of highly borated fluid into the (still solid, i.e. not yet  
 1226 vaporized liquid in the moderator tank at the concerned time) affects the FPP. A top view picture for  
 1227 boron arrival into the moderator tank and consequent boron cloud formation is provided in the  
 1228 bottom of Fig 20 (left and tight sketches correspond to two different times)

1229 A complex modeling activity was needed to calculate (a) BIT (this took benefit from the already  
 1230 mentioned BITF experiment, [Moretti et al., 2018](#)), (b) the borated fluid diffusion (this needed CFD  
 1231 analyses), and (c) the impact of local poisoned moderator upon FPP generated by void formation.  
 1232 A detailed three-dimensional coupled thermal-hydraulics and neutron physics calculation was  
 1233 carried out considering local values for coolant and moderator fluid parameters, primarily  
 1234 temperature and void, and for nuclear fuel, primarily burn-up and pin temperature distribution.  
 1235 Selected results are shown in Fig. 21, also supported by MCNP calculations, [Pecchia et al., 2009](#), and  
 1236 [Pecchia et al., 2015](#). Calculated FPP is about 10 times the nominal power and occurs before 1.0 s (top  
 1237 left); power distribution at the time of PCT is given in the top right diagram. The time change in axial  
 1238 power profile for individual fuel assemblies can be seen in each of the bottom diagrams; the different  
 1239 behavior power profiles evolutions between two different fuel channels can be noted.  
 1240



1241



1242

1243 **Figure 21.** Atucha-II LBLOCA, evaluation of FPP. Top: overall core power. Bottom: power profile  
 1244 during the FPP in different fuel channels.

1245 4.3.3 The Overall System Performance (PHW 1, 2 and 3)

1246 4.3.3.1. Key Variables

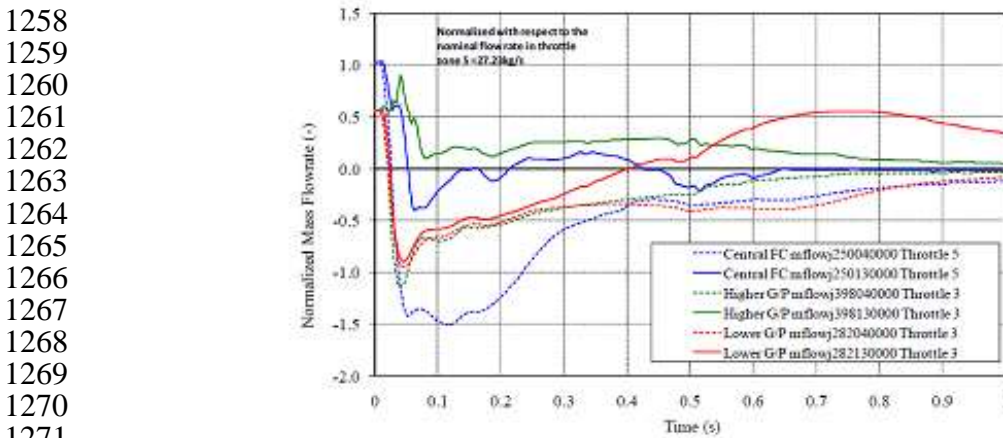
1247 The qualitative global LBLOCA scenario in Atucha-II PHWR is the same as a typical PWR, as  
 1248 already mentioned: in other terms, from a qualitative viewpoint, the time trends of pressure in RPV,  
 1249 in pressurizer, in steam generator secondary side and in containment, of mass inventory in RPV and

1250 of rod surface temperature experiencing CHF, PCT and reflow, are similar. Emphasis is given below  
1251 to the description of a few selected differences between Atucha-II PHWR and PWR.

#### 1252 4.3.3.2. Flow Reversal at Core Inlet

1253 The low amount of fluid mass in the case of Atucha-II (related to a typical PWR) in lower  
1254 plenum and the geometric diameter of the core cause, see Fig. 22:

- 1255 ○ Early core flow reversal.
- 1256 ○ Low influence of lower plenum flashing.
- 1257 ○ Differences in flow reversal as far as individual channel locations are concerned.

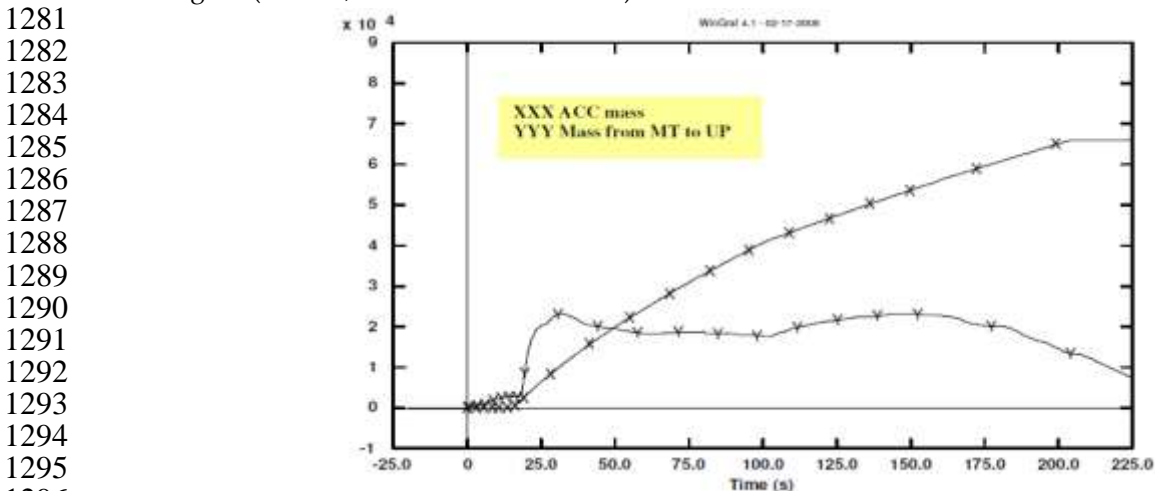


1272 **Figure 22.** Atucha-II LBLOCA, occurrence of flow reversal at fuel channel inlets.

#### 1273 4.3.3.3. The ECCS and the Moderator Performance.

1274 ECCS consisting of accumulator and LPIS (also called SIP, see Table 1), deliver mass flowrates  
1275 in both CL and HL. ECCS delivered mass becomes equal to break mass flow roughly at the time of  
1276 pressure equalization between primary system and containment (Table 4).

1277 The special role of moderator cooling loops should be considered. During nominal operation the  
1278 four moderator circuits remove about 10% of core power (see also Table 1). During LBLOCA  
1279 transient an intrinsic and a design role in cooling the core can be seen from Fig. 23 (PHW 2 and 3)  
1280 and Fig. 25 (PHW 4, see section 4.3.5 below).



1297 **Figure 23.** Atucha-II LBLOCA: moderator cooling by liquid delivery in core region (PHW 2 and 3).

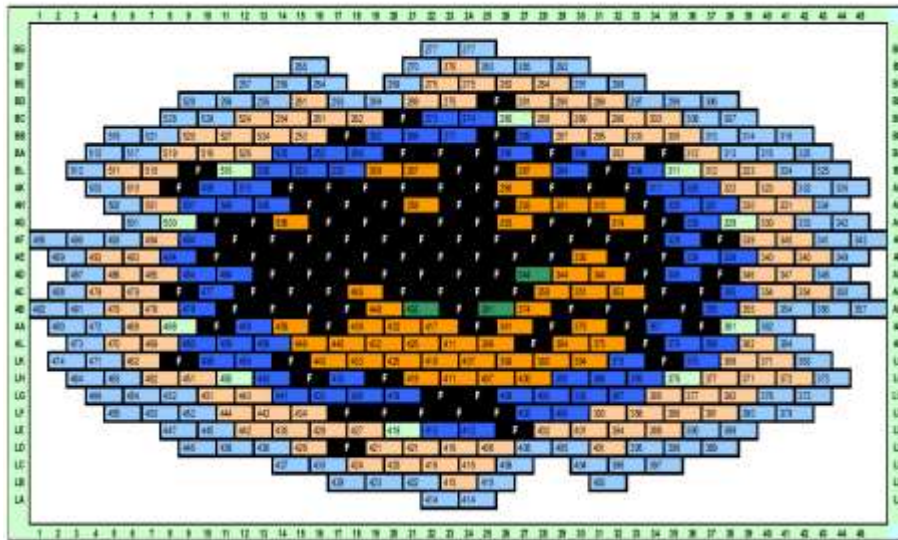
1298 The mass flowrate from moderator tank towards the upper parts of fuel channels, which  
1299 experience a pressure lower than the moderator tank pressure owing to the break in the primary  
1300 loop, is given in Fig. 23 (vertical axis); a comparison is made in the same figure with the accumulator



1301 mass delivered from the HL region: an early contribution of moderator liquid to core cooling during  
1302 PHW 2 and PHW 3 can be noted.

1303 4.3.4 Nuclear Fuel Performance (PHW 3)

1304 Evaluation of fuel failures constituted an essential part of the LBLOCA analysis because of the  
1305 need to estimate radioactivity release. A complex pattern for fuel failure was established including  
1306 ballooning and consequent bursts, Adorni et al., 2011; H<sub>2</sub> production and clad fragility were  
1307 calculated. The result is a fuel failure map, Fig. 24; fuel channels including at least one failed rod are  
1308 shown in black. The exact number of fuel rod failed was used to calculate radiological release.



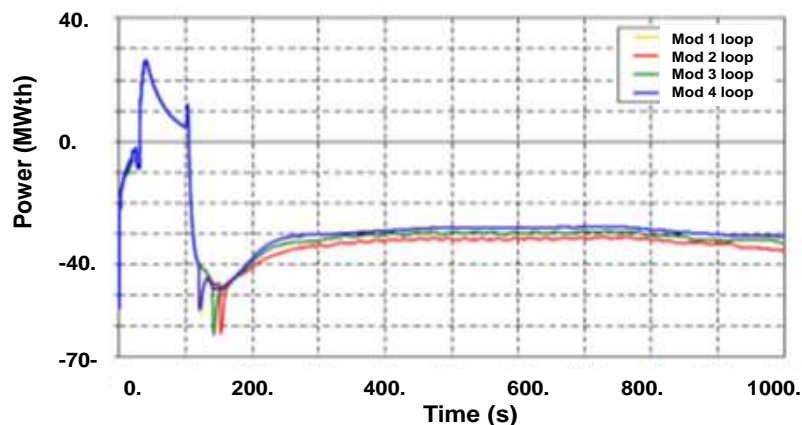
1327 **Figure 24.** Atucha-II LBLOCA: resulting fuel failure map shown in a core cross-section.

1328 4.3.5. Long Term Cooling, Containment Behavior, Radioactivity in the Environment (PHW 4)

1329 A key question to be answered for LTC analysis is “At what time the calculation must be  
1330 extended?” The answer needs a phenomena evaluation (i.e. demonstration that core cooling  
1331 conditions are stable) and a connection with licensing needs. Half-a-hour after the event start was  
1332 considered a suitable compromise in the case of Atucha-II LBLOCA.

1333 4.3.5.1. Moderator Role During LTC

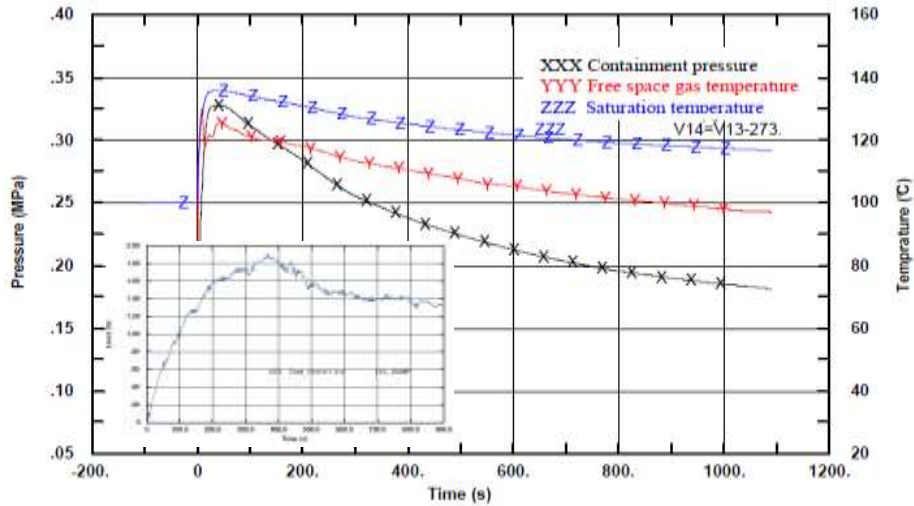
1334 The moderator cooling loops include heat exchangers which in case of LOCA are connected  
1335 with outside of containment and are capable of removing thermal power according to Fig. 25.



1351 **Figure 25.** Atucha-II LBLOCA: thermal power removal from core by moderator loops (PHW 4).

1352 4.3.5.2. Containment, Sump Recirculation and Debris

1353 In the case of Atucha-II LBLOCA BEPU analysis both containment and containment annulus (or  
 1354 the region between the pressure 'containment sphere', see Table 1, and the reactor building) were  
 1355 modeled and (fully) coupled to primary cooling and moderator systems. Pressure and fluid  
 1356 temperatures were calculated together with sump level, Fig. 26.

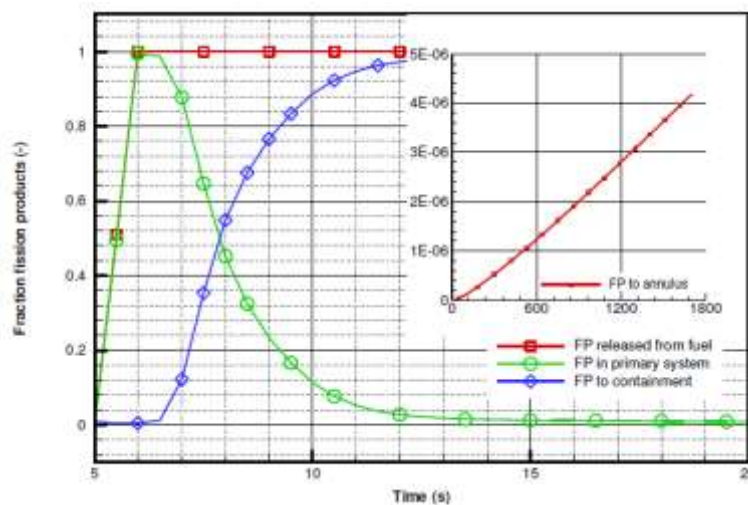


1373 **Figure 26.** Atucha-II LBLOCA: containment pressure and temperature and sump level.

1374 The sump level (diagram at bottom left of Fig. 26) and the liquid temperature in the sump (not  
 1375 shown in the figure) allowed the demonstration of consistency with the Net Positive Suction Head  
 1376 (NPSH) of pumps used for LTC. Margins to available NPSH for debris effects were considered  
 1377 although, consistently with state of art, properly designed grids were installed in the sump.

1378 4.3.5.3. Radioactivity Release

1379 The main goal for the overall LBLOCA analysis consisted in the calculation of doses external to  
 1380 the reactor building under identified atmospheric conditions at an assigned distance. This implied  
 1381 'deterministic' calculation of: a) fuel damage (section 4.3.4); b) radioactivity leaking from fuel; c)  
 1382 radioactivity diffusion in the primary loop; d) radioactivity ending into the containment; e) based on  
 1383 containment pressure and leaking test data, radioactivity into the reactor building (or the annular  
 1384 space of containment); f) radioactivity exiting the reactor building; g) doses at the assigned position  
 1385 for the assigned time duration. Indicative results from steps b), c), d) and e) are provided in Fig. 27.



1402 **Figure 27.** Atucha-II LBLOCA: radiation release from damaged fuel ending into the primary loop,  
 1403 containment and reactor building.

1404 Distinguishing about several release categories, and considering different transport  
1405 mechanisms allowed the calculation of the activity expected at the given location external to the  
1406 reactor building. The additional (regulatory) assumption about persons absorbing the radiation  
1407 allowed the calculation of doses (overall result given at line 29 in Table 4).

#### 1408 4.4. The Application of BEPU

1409 The framework and the role of BEPU can be derived from chapter 1 and section 3.6 above.  
1410 Atucha-II licensing process brought to a cornerstone in the history of BEPU as it happened, roughly  
1411 one decade before, with Angra-2 licensing process in Brazil. Namely, both Angra-2 and Atucha-II  
1412 constituted the first reactor put in operation based on the application of a BEPU approach to  
1413 LBLOCA and to all the entire spectrum of accidents, respectively.

#### 1414 4.4.1 The BEPU Approach in Atucha-II Licensing

1415 The availability and the handling capability for a series of codes (a couple dozen adopted, not  
1416 listed here) and the availability of an uncertainty method, see [D'Auria & Giannotti, 2000](#), and  
1417 [Petruzzi & D'Auria, 2006](#), constituted prerequisites for BEPU application. This is discussed in the  
1418 proprietary document [Muellner et al., 2008](#), and synthesized by [D'Auria & Mazzantini, 2009](#), see also  
1419 [D'Auria et al., 2012](#). Even a summary description is outside the framework for the present paper;  
1420 rather the main challenges for BEPU application to Atucha-II licensing are listed below.

- 1421 ⇒ Full BEPU analyses were performed for the entire spectrum of accidents. In some cases,  
1422 following criteria agreed with the Regulatory Body (i.e. when wide safety margins were  
1423 calculated), uncertainty analyses were not documented in the Final Safety Analysis Report.  
1424 For instance, it was checked for each concerned transient analysis (i.e. when uncertainty  
1425 results are not documented), that uncertainty contribution did not bring to CHF if CHF was  
1426 not part of the original BE calculation result.
- 1427 ⇒ The LBLOCA challenges (see section 4.2) also constitute BEPU challenges.
- 1428 ⇒ Each design peculiarity of Atucha-II, or the difference between PWR and PHWR (use of  
1429 D2O, continuous fuel reload, etc.), was at the origin of a challenge for the BEPU approach  
1430 which had been developed and previously qualified for PWR applications.
- 1431 ⇒ The detailed consideration of I & C interaction with operation and safety of the reactor, or I  
1432 & C modeling, was needed, e.g. starting from the fine movement of control rods to adjust  
1433 the local neutron flux and going to the control of turbine flow and moderator fluid  
1434 temperature.
- 1435 ⇒ Adoption of conservatism was of no help (and no support) to justify BEPU results; e.g. use  
1436 of conservative input for predicting FPP would imply unacceptable results: this actually  
1437 imposed BEPU as the only way to evaluate Atucha-II safety.
- 1438 ⇒ The licensing connection implied consideration of regulatory documents in both the  
1439 Countries where the reactor was designed (Germany) and constructed (Argentina);  
1440 furthermore, USNRC rules (see also below) had to be considered.
- 1441 ⇒ The fundamental (and somewhat philosophical) safety concept of 'single failure' was  
1442 considered, notwithstanding the Best Estimate (or realistic) nature of the analysis, i.e.  
1443 connected with physical phenomena evaluation: the difficulty is associated with (not only in  
1444 case of LBLOCA study) the need to identify the most effective failing component (among  
1445 several thousand part of I & C).
- 1446 ⇒ Because of the pioneering (BEPU) approach, an international group of experts was formed  
1447 under the supervision of the Regulatory Body in Argentina: the BEPU approach, [Muellner et  
1448 al., 2008](#), and the results from the BEPU application, [GRNSPG, 2010](#), were thoroughly  
1449 reviewed and generated series of mandatory questions which needed further analyses.

#### 1450 4.4.2. Selected Validation And Uncertainty Steps and Results

1451 A few BEPU-LBLOCA related topics (i.e. a narrow view over a universe of BEPU supporting  
1452 activities) are described below in order to provide, as far as possible, an idea of the performed  
1453 investigations.

#### 1454 4.4.2.1. Development of Atucha-II Model (Nodalizations)

1455 The nodalization, or input deck, is the interface between the numerical code and the reactor  
 1456 design and operation; the nodalization must account for the objective of the analysis although a  
 1457 unique 'general purpose' input deck suitable for all transient analysis was developed. In order to  
 1458 acquire confidence of the results and get suitable quality from the analyses, at least six main  
 1459 nodalizations were developed, here distinguished by the number of radial regions adopted to  
 1460 simulate the Atucha-II core: 1, 2, 36, 60, 280 and 451 core regions were built. The last one implied  
 1461 each individual channel separately modeled, a full three-dimensional model for the RPV and up to  
 1462 ten thousands nodes for the primary system.  
 1463 Convergence of results when increasing number of core channels from 1 to 451 was not achieved, as  
 1464 expected; however, discrepancies among calculations from various input decks were explained and  
 1465 helped in removing errors and constituted a support for the final 'licensing' result.

1466 4.4.2.2. Nodalization Qualification, Kv-Scaled Analyses

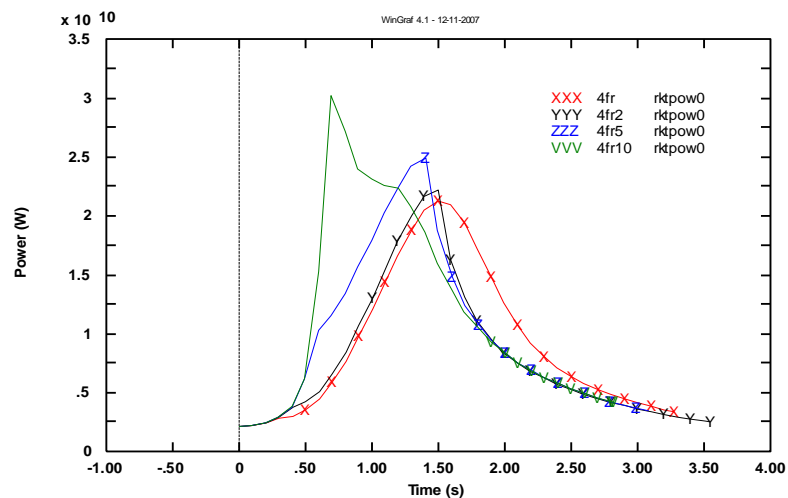
1467 Established procedures were used to qualify each developed nodalization (i.e. whatever the  
 1468 number of modeled core channels, see above), [Bonuccelli et al., 1993](#). A noticeable step in the process  
 1469 is the Kv-scaled analysis already introduced in 1995, [D'Auria et al., 1995](#). A step of the procedure  
 1470 implies the comparison between a calculated Atucha-II and a measured Accident Scenario (AS) in  
 1471 any PWR experimental test facility (ITF). Obviously difference are expected and occur between the  
 1472 AS datasets. The activity consists in demonstrating, by performing additional calculations:

- 1473 • the reason of each difference,
- 1474 • that geometry and initial conditions are the origin of the difference,
- 1475 • that phenomena not measured in the ITF do not results from Atucha-II AS.

1476 In recent years it was also shown by [OECD/NEA/CSNI, 2017](#) that the so-called triad method,  
 1477 [Ransom et al., 1998](#), consists of elements part of Kv-scaled procedure. Within the same international  
 1478 document the use of the methods (either Kv-scaled or triad) is recommended for addressing the  
 1479 scaling issue.

1480 4.4.2.3. Convergence of Results When Varying Time Steps

1481 As expected, reducing the time step, whatever the starting nodalization, did not bring to  
 1482 convergence of results, see e.g. Fig. 28; in general terms decreasing of time steps and increasing the  
 1483 number of nodes (or reducing the node size, see also above) for the primary system of Atucha-II did  
 1484 not bring to convergence of results. This put an additional challenge to the application of BEPU and  
 1485 needed a number of sensitivity studies supported, whenever possible, by experimental evidence.

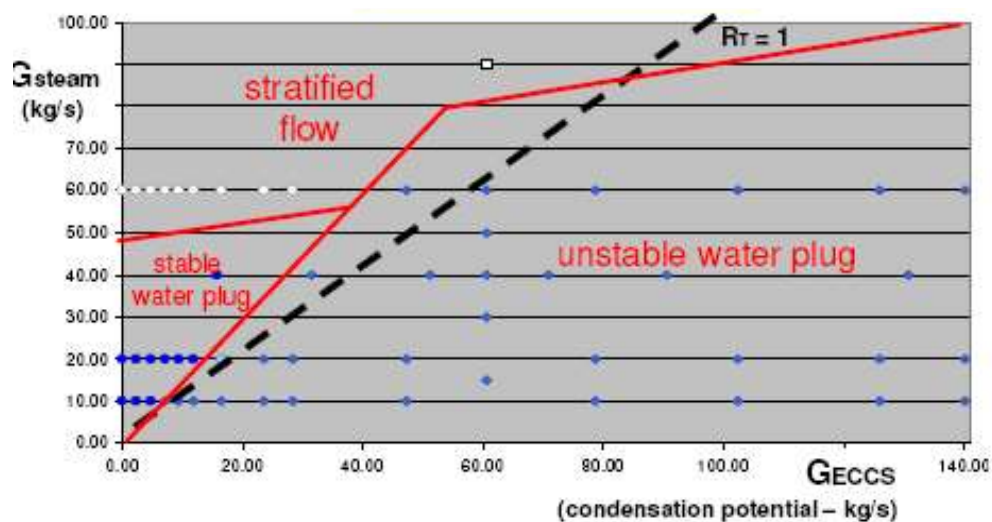


1502 **Figure 28.** Atucha-II LBLOCA: FPP calculated by different time steps and different nodalizations (the  
 1503 highest peak on the left resulting from the smallest time step).

1504 Convergence and realism of final results was demonstrated making use of experimental data in the  
 1505 case of thermal-hydraulic parameters: an example can be found in the paper by [Lazarte & Ferreri,](#)  
 1506 [2012](#), dealing with natural circulation. In the case of neutron flux data and fission power, the  
 1507 calculation results derived from CANDU analyses, see [Kastanya et al., 2013](#) (e.g. duration and  
 1508 amplitude of power peak resulting from void reactivity), were considered.

#### 1509 4.4.2.4. Thermal-Hydraulic Code Specific Validation and Applicability

1510 Question marks were raised at different steps of the BEPU process in relation to the capabilities  
 1511 of adopted codes to reproduce the AS phenomenology expected in Atucha-II. For instance, the  
 1512 challenge [9] in section 4.2 (CCFL in HL) may appear in any PWR; however in the case of the  
 1513 Atucha-II system, the ratio between flow area of HL and the volumetric steam flow produced in the  
 1514 core (originated by decay power) achieves a minimum value, thus generically requesting higher  
 1515 precision of results and higher confidence towards results. The CCFL issue was of primary concern  
 1516 for the 0.1 A break LOCA analysis. This imposed a pioneering (in the sense of not available before)  
 1517 demonstration of capability for the adopted code version: all experimental data measured in UPTF,  
 1518 were collected to form different regions in a suitable phase space. Applicability of the code and of  
 1519 the adopted nodalization details was confirmed, Fig. 29, and used for the present LBLOCA analysis  
 1520 (for more details of the experimental data base see also the paper [Rohatgi & Glaeser, 2019](#), in this  
 1521 Special Issue).



1539 **Figure 29.** Atucha-II LBLOCA: comparison between measured and calculated CCFL regimes in  
 1540 UPTF.

#### 1541 4.4.2.5. Selected Miscellaneous Findings or Outcomes from the BEPU Process

- 1542 A few statements below provide further views of the performed BEPU application.
- 1543 1) Sensitivity analyses were systematically adopted, not only to deal with convergence of  
 1544 results, but also to support uncertainty evaluation.
  - 1545 2) Two uncertainty methods (independent among each other) were used to increase the  
 1546 confidence in establishing safety margins in some situations (e.g. evaluation of FPP).
  - 1547 3) A full three-dimensional model for thermal-hydraulics and neutron physics was needed to  
 1548 demonstrate the safety of the large and low power density (in terms of kw/l) core: different  
 1549 core regions contribute to phenomena (like the FPP) at different times, making unrealistic  
 1550 any more simplified approach (e.g. 0-D, 1-D, etc.).
  - 1551 4) Computational Fluid Dynamics (CFD) and Montecarlo type of numerical codes (MCNP)  
 1552 were strictly needed to perform analyses supporting the application of a coupled 3-D  
 1553 thermal-hydraulic and neutron physics model.
  - 1554 5) About five hundred documents were produced to address any question raised during the  
 1555 BEPU process.

1556 6) A specific Data Management System was adopted to manage the data resulting from the  
1557 analysis and for issuing the FSAR (about one thousand sections, all together).

1558

## 1559 5. Conclusions

1560 A brief historical overview is introduced in the paper to connect the thermal-hydraulic design  
1561 of the Atucha-II PHWR with a PWR. Key complexities of both systems are compared: basically, the  
1562 CANDU features of using natural uranium and heavy water as moderator are associated in the case  
1563 of Atucha-II with the presence of the pressure vessel typical of PWR. Then, LBLOCA evolution (in  
1564 Atucha-II) has several similarities with the widely investigated and well understood LBLOCA in  
1565 PWR with one significant difference: the fission power excursion which occurs during the early  
1566 blowdown period which impacts the PCT and the fuel safety margins. A LOCA-RIA transient  
1567 occurs. This was one main trigger and motivation for the performed activity.

1568 Atucha-II licensing process was completed in 2014 at the time when the reactor unit was  
1569 connected to the electrical grid. The BEPU approach has been used to issue the Chapter 15 of the  
1570 FSAR and a wide range investigation was completed to deal with the LBLOCA (or 2A, or 2 x 100%  
1571 A, or DEGB).

1572 The application of BEPU was unavoidable to avoid the use of conservatism: one may state that  
1573 the modeling of neutron interaction with the materials in the core and the geometric and operating  
1574 conditions of the reactor brought to the calculation of fission power peak and to demonstration of  
1575 Atucha-II safety margins: i.e. no conservative or designer suggested parameter value was adopted to  
1576 achieve such demonstration.

1577 A wide variety of challenges (some of those listed in the paper) had to be addressed; these were  
1578 solved by searching for the availability of experimental data with the support of sensitivity studies  
1579 and adopting a couple dozen qualified numerical tools. Actually an important challenge was  
1580 constituted by inadequacies of computational tools.

1581 The PWR Large Break Loss of Coolant Accident scenario has been revisited in the occasion of  
1582 summarizing the results from BEPU analysis of LBLOCA in Atucha-II PHWR.

1583 Key findings of technological interest from the performed LBLOCA analysis are:

- 1584 • The LBLOCA has direct impact upon the overall design of PWR (and PHWR), including the  
1585 layout of the primary loop: suitable safety analyses shall not ignore the importance of  
1586 LBLOCA also to avoid loss in credibility towards the technology of (high pressure) water  
1587 cooled nuclear reactors.
- 1588 • The nuclear fuel weaknesses which have been recently characterized from measurements of  
1589 irradiated rods may have a limited impact upon Atucha-II safety evaluations because of the  
1590 relatively low burn-up which characterizes the operation of PHWR; rather the discovery of  
1591 fuel weakness may need significant changes in regulations.
- 1592 • The role of containment as the key barrier to the release of fission products is directly  
1593 reflected by current Argentinean regulations: fuel failures and radioactivity releases into the  
1594 containment can be tolerated from the analyses of events part of DBA provided suitable  
1595 thresholds are fulfilled for the radioactivity into the environment. The philosophy at the  
1596 basis of the Argentinean regulations, outlined in this paper, can be pursued at the  
1597 international level.
- 1598 • The amplitude of the depressurization wave generated at the break is a function of the Break  
1599 Opening Time (BOT): notwithstanding fundamental research and technological  
1600 achievements in the area of the LBB an acceptable (regulatory) justification for BOT longer  
1601 than a few m-s could not be found.
- 1602 • BOT in the order of 1 s and/or increase in initial break flow (justified in Atucha-II by the  
1603 special configuration of the nozzle connecting the CL to the RPV) brings to substantial  
1604 reduction in the value of FPP: neither of those two circumstances has been considered in the  
1605 licensing process.
- 1606 • Loads upon internals and early vaporization in individual fuel channels generated by the  
1607 pressure wave have been calculated by three dimensional techniques. Acceptable  
1608 mechanical stresses and subsequent voiding of different core regions bringing to a

1609 smoothed FPP (i.e. compared with the case of simultaneous voiding of the entire core) have  
 1610 been calculated.

- 1611 • Lack of convergence in either space or time, i.e. results of code calculations do not converge  
 1612 when the time steps and the node sizes are reduced, constitutes a deficiency of current  
 1613 computational tools and a challenge for the (BEPU) analyses. Supporting analyses and  
 1614 experimental data (namely in the area of transient thermal-hydraulics) were considered in  
 1615 order to minimize the impact of lack of convergence; uncertainty evaluation (embedded into  
 1616 the BEPU process) accounted for the expected residual error.
- 1617 • Procedures adopted within the concerned Atucha-II licensing process, e.g., noticeably, the  
 1618 Kv-scaled calculation to address the scaling issue, were internationally recognized as  
 1619 essential elements of BEPU applications.
- 1620 • The construction and the operation of the BITF experimental test facility (scale 1:1) to  
 1621 demonstrate the compliance of Boron Injection Time (BIT) with the calculated value shall be  
 1622 seen as a valuable example of the interaction between safety requirements, reactor design  
 1623 and research needs coming from BEPU application.

1624 The Atucha-II licensing by BEPU (entire Chapter 15) constituted at the same time a pioneering  
 1625 effort and a cornerstone in the application of BEPU. This was possible thanks to the availability of  
 1626 Regulators and the thrust towards science, technology and innovation by the utility (plant owner) in  
 1627 Argentina. International community, particularly IAEA, looked positively at the overall initiative.  
 1628 Definitely, the frontier of numerical code application and suitability, not only in the area of  
 1629 thermal-hydraulics, has been progressed by BEPU application in the licensing process of Atucha-II  
 1630 NPP.

### 1632 **Acknowledgements**

1633 *First acknowledgement here is for J. L. Antunez: during the period of execution of the present activity he was the Project*  
 1634 *Director for Atucha-II, later on he became President of NA-SA: he is an illuminated scientist who, other than being able to*  
 1635 *bring to a positive end an extremely complex endeavor like the construction of Atucha-II, directed 'behind the scene' the*  
 1636 *cooperation between University of Pisa and NA-SA. Thanks are due to International Review Group members N. Aksan, C.*  
 1637 *Camargo, M.R. Galetti, N. Fil, K. Ivanov, and L. Leung. At University of Pisa responsible scientists for individual activities*  
 1638 *were N. Muellner, A. Petruzzi, M. Cherubini, W. Giannotti, C. Parisi, F. Moretti, D. Melideo, F. Terzuoli, A. Del Nevo,*  
 1639 *G.M. Galassi, M.C. Galassi, M. Giersch, D. Araneo, M. Lanfredini, N. Arnold, M. Adorni, P. Pla, and D. Lazzarini. At*  
 1640 *NA-SA responsible scientists were M. Schivo and A. Bonelli.*

### 1642 **LIST OF ACRONYMS**

1643	A	Flow Area (typically of CL or HL)
1644	AA	Accident Analysis
1645	ACC	Accumulator
1646	APW	Amplitude of Pressure Wave
1647	ARN	Regulatory Body in Argentina
1648	AS	Accident Scenario
1649	BA	Break Area
1650	BAF	Bot of Active Fuel
1651	BEPU	Best Estimate Plus Uncertainty
1652	BIT	Boron Injection Time (= time for Boron to arrive in the MOD after the signal)
1653	BITF	Boron Injection test Facility
1654	BOT	Break Opening Time
1655	BP	Break Position
1656	CANDU	Canadian Deuterium Uranium (reactor)
1657	CC	Central Channel
1658	CCFL	Counter Current Flow Limitation
1659	CFD	Computational Fluid Dynamics
1660	CHF	Critical Heat Flux
1661	CL	Col Leg
1662	CRDM	Control Rod Drive Mechanism
1663	CVR	Core Void Reactivity
1664	DBA	Design Basis Accident
1665	DC	Downcomer
1666	DEGB	Double Ended Guillotine Break

1667	DNB	Departure from Nucleate Boiling
1668	ECC	See ECCS
1669	ECCS	Emergency Core Cooling System (see also ECC)
1670	ESF	Engineered Safety Features
1671	FA	Fuel Assembly
1672	FC	Fuel Channel
1673	FPP	Fission Power Peak (lower than TPP)
1674	FSAR	Final Safety Analysis Report
1675	FW	Feed Water
1676	G/P	Mass flow-rate divided by power in each FA
1677	HEX	Heat Exchanger
1678	HL	Hot Leg
1679	IGSCC	Inter Granular SCC
1680	I&C	Instrumentation and Control (system)
1681	KWU	NPP Designer in Germany
1682	LBB	Leak Before Break
1683	LBLOCA	Large Brea LOCA
1684	LHGR	Linear Heat Generation Rate
1685	LOCA	Loss of Coolant Accident
1686	LP	Lower Plenum
1687	LPIS	Low Pressure injection System (see also SIP)
1688	LPZ	Low Population Zone
1689	LTC	Long Term Cooling
1690	LVL	Level
1691	MCP	Main Coolant Pump
1692	MOD	Moderator
1693	MT	Moderator Tank
1694	NPP	Nuclear Power Plant
1695	NPSH	Net Positive Suction Head
1696	NRS	Nuclear Reactor Safety
1697	NA-SA	NPP Utility in Argentina
1698	PCCI	Pellet Clad Chemical Interaction
1699	PCMI	Pellet Clad Mechanical Interaction
1700	PCT	Peak Clad Temperature
1701	PHW	Phenomenological Window (also Ph.W)
1702	PHWR	Pressurized Heavy Water Reactor
1703	PRZ	Pressurizer
1704	PS	Primary System
1705	PWR	Pressurized Water Reactor
1706	PWSCC	Primary Water SCC
1707	QF	Quench Front
1708	RCS	Reactor Coolant System
1709	RIA	Reactivity Initiated Accident
1710	RIH	Reactor Inlet Header
1711	RNB	Return to Nucleate Boiling
1712	RPV	Reactor Pressure Vessel
1713	SCC	Stress Corrosion Cracking
1714	SG	Steam Generator
1715	SIP	Safety Injection Pump (see also LPIS)
1716	TAF	Top of Active Fuel
1717	TPCF	Two Phase Critical Flow
1718	TPP	Total Power Peak (higher than FPP)
1719	UP	Upper Plenum
1720	USAEC	Regulatory Authority in US
1721	USNRC	Regulatory Authority in US
1722	V&V	Verification and Validation
1723	WWII	Second World War
1724		
1725	<b>References</b>	



1726  
1727  
1728  
1729  
1730  
1731  
1732  
1733  
1734  
1735  
1736  
1737  
1738  
1739  
1740  
1741  
1742  
1743  
1744  
1745  
1746  
1747  
1748  
1749  
1750  
1751  
1752  
1753  
1754  
1755  
1756  
1757  
1758  
1759  
1760  
1761  
1762  
1763  
1764  
1765  
1766  
1767  
1768  
1769  
1770  
1771  
1772  
1773  
1774  
1775  
1776  
1777  
1778  
1779  
1780  
1781  
1782  
1783  
1784

Adorni M., Del Nevo A., D'Auria F., Mazzantini O., 2011, A Procedure to Address the Fuel Rod Failures during LB-LOCA Transient in Atucha-2 NPP, *J. Science and Technology of Nuclear Installations*, Article ID 929358, ISBN 1687-6075, doi 10.1155/2011/929358, pages 1-7

Aksan N., D'Auria F., Groeneveld D., Kirillov P., Saha D., Badulescu A., Cleveland J., (Lead Authors), 2001, *Thermo-hydraulic Relationships for Advanced Water Cooled Reactors*", IAEA TECDOC 1203, April, Vienna (A), ISSN 1011-4289, pp 1-344

Aksan S. N., 2017, Target phenomena in nuclear thermal-hydraulics, Book 'Thermal Hydraulics in Water-Cooled Nuclear Reactors', [F. D'Auria, Editor], Chapter 15, Elsevier, Woodhead Publishing, ISBN 9780081006627, pp 245-356

Aksan N., D'Auria F., Glaeser H., 2018, Thermal-hydraulic phenomena for water cooled nuclear reactors, *Nuclear Engineering and Design*, 330, pp 166-186

Ammirabile L., Walker S.P., 2014, Dynamic ballooning analysis of a generic PWR fuel assembly using the multi-rod coupled MATARE code, *Nuclear Engineering and Design*, 268, 24-34

Ashley R., El-Shanawany M., Eltawila F., D'Auria F., 1998, Good practices for user effect reduction, OECD/NEA/CSNI report NEA/CSNI/R(98)22, Paris, France

Azam M.S., Niu F., Wang D., Zhuo W., 2018, Experimental and CFD analysis of the effects of debris deposition across the fuel assemblies, *Nuclear Engineering and Design*, 332, 238-251

Baum M. R., 1984, Break opening times for axial ruptures of a gas-pressurized pipe, *Nuclear Engineering and Design*, 77, 161-167

Bhandari S., Leroux J.C., 1993, Evaluation of crack opening times and leakage areas for longitudinal cracks in a pressurized pipe Part II. Application of proposed model and fracture dynamics, *Nuclear Engineering and Design*, 142, 21-25

Bianco A., Vitanza C., Seidl M., Wensauer A., Faber W., Macián-Juan R., 2015, Experimental investigation on the causes for pellet fragmentation under LOCA conditions, *Nuclear Materials*, 465, 260-267

Bonelli A., Siefken L., Mazzantini O., Allison C., 2014, Summary of Severe Accident Assessment for Atucha 2 Nuclear Power Plant using RELAP5/SCDAPSIM Mod3.6 , 10<sup>th</sup> Int. Top. Meet. on Nuclear Thermal-Hydraulics, Operation and Safety (NUTHOS-10), NUTHOS10-1128, Dec. 14-18, Okinawa, Japan

Bonuccelli M., D'Auria F., Debrecin N., Galassi G.M., 1993, A methodology for the qualification of thermal-hydraulic codes nodalizations, Int. Top. Meet. on Nuclear Reactor Thermal-Hydraulics (NURETH-6), Grenoble, France

Bourga R., Moore P., Janin Y-J., Wang B., Sharples J., 2015, Leak-before-break: Global perspectives and procedures, *Int. J. of Pressure Vessels and Piping*, 129-130, 43-49

Bousbia Salah A., Vedovi J., D'Auria F., Ivanov K., Galassi G.M., 2004, Analysis of the Peach Bottom Turbine Trip 2 Experiment by coupled Relap5-Parcs three dimensional codes, *Nuclear Science and Engineering*, 148, 337-353

Brankov V. V., 2017, Modelling of fuel fragmentation, relocation and dispersal during Loss-of-Coolant Accident in Light Water Reactor, PHD These No 8018, École Polytechnique Fédérale de Lausanne (CH)

Brittain I., Aksan N., 1990, OECD-LOFT Large Break LOCA Experiments Phenomenology and Computer Code Analyses, AEA-TRS-1003, PSI Report 72, Wurenlingen / Villigen, (CH)

Celata G. P., Cumo M., D'Annibale F., Farello G. E., 1986, Two-phase flow models in unbounded two-phase critical flow, *Nuclear Engineering and Design*, 97, 211-222

1785 Chatzikiyriakou D., Walker S.P., Hewitt G. F., 2010, The contribution of non-wetting droplets to direct cooling of  
1786 the fuel during PWR post-LOCA reflood, *Nuclear Engineering and Design*, 240, 3108–3114  
1787  
1788 Chun M-H., Yu S-O., 2000, Effect of steam condensation on countercurrent flow limiting in nearly horizontal  
1789 two-phase flow, *Nuclear Engineering and Design*, 196, 201-217  
1790  
1791 Collier J.G., 1975, *Two Phase Flow and Heat Transfer in Water Cooled Nuclear Reactors*, Lecture Series,  
1792 Dartmouth College, New Hampshire, USA  
1793  
1794 Damerell P. S., Simons J. W. (Eds.), 1993, *Reactor Safety Issues Resolved by the 2D/3D Program*, MPR  
1795 Associates, Inc., GRS-101, ISBN 3-923875-51-7, Sept.  
1796  
1797 D'Auria F., Vigni P., 1981, Fluid-dynamic Analysis of Steam-Water Flows from a Pressure Vessel, Workshop on  
1798 Jet Impingement and Pipe Whip, June 29 - July 1, Genova (I)  
1799  
1800 D'Auria F., Vigni P., 1989, Evaluation of Fluid-dynamic Loads on RPV Internals during Blowdown, 10<sup>th</sup> SMIRT  
1801 Int. Conf., Aug. 14-18, Anaheim (CA, USA)  
1802  
1803 D'Auria F., Debrecin N., Galassi G.M., 1995, Outline of the uncertainty methodology based on accuracy  
1804 extrapolation (UMAE), *Nuclear Technology* 109, 1  
1805  
1806 D'Auria F., Galassi G.M., 1998, Code validation and uncertainties in system thermalhydraulics, *Progress*  
1807 *Nuclear Energy*, 33 (1/2), 175–216  
1808  
1809 D'Auria F., Giannotti W., 2000, Development of Code with capability of Internal Assessment of Uncertainty,  
1810 *Nuclear Technology*, 131, 1, 159-196,  
1811  
1812 D'Auria F., Mazzantini O., Cherubini M., Giannotti W., Parisi C., Moretti F., Melideo D., Del Nevo A., Galassi  
1813 G.M., Araneo D., Terzuoli F., Adorni M., Muellner N., Petrucci A., Lazzerini D., Santoro R., Bousbia-Salah A.,  
1814 2008, DEGB LBLOCA (2 X 100% Break in CL) in Atucha-2 NPP, University of Pisa Report, DIMNP NT 628(08) –  
1815 rev.1, Pisa (I), March – Delivered to NA-SA, Buenos Aires (Arg), pp 1-259  
1816  
1817 D'Auria F., Mazzantini O., 2009, The Best-Estimate Plus Uncertainty (BEPU) Challenge in the Licensing of  
1818 Current Generation of Reactors, Int. Conf. on Opportunities and Challenges for Water Cooled Reactors in the  
1819 21<sup>st</sup> Century, IAEA, Oct. 27-30, Vienna (A)  
1820  
1821 D'Auria F., Camargo C., Mazzantini O., 2012, The Best Estimate Plus Uncertainty (BEPU) approach in licensing  
1822 of current nuclear reactors, *Nuclear Engineering and Design*, 248, 317-328  
1823  
1824 D'Auria F., Galassi G. M., 2017, Applications of SYS TH codes to nuclear reactors designs and accident analysis,  
1825 Book 'Thermal Hydraulics in Water-Cooled Nuclear Reactors', [F. D'Auria, Editor], Chapter 15, Elsevier,  
1826 Woodhead Publishing, ISBN 9780081006627, pp 951-1098  
1827  
1828 D'Auria F., Lanfredini M., 2018, Introducing V&V&C in nuclear thermal-hydraulics, ASME Verification and  
1829 Validation Symposium (VVS2018-9321), May 16-18, Minneapolis (Mn, US)  
1830  
1831 D'Auria F., 2018, BEPU status and perspectives, Invited at ANS Best Estimate plus Uncertainty Int. Conf.  
1832 (BEPU2018), May 13-18, Lucca (I), PL10  
1833  
1834 D'Auria F., Debrecin N., Glaeser H., 2018, New Safety Barrier for current and future nuclear reactors, Invited at  
1835 V Int. Scientific and Technical Conf. <Innovative Design and Technologies of Nuclear Power>, V ISTC NIKIET,  
1836 Oct. 2-5, Moscow (Ru), ISBN 978-5-98706-120-6  
1837  
1838 D'Auria F., Debrecin N., Glaeser H., 2019, The need for an additional technological safety barrier for current and  
1839 future NPP, Invited at Int. Conf. on Nuclear Power Plants, Structures, Risk & Decommissioning (NUPP2019),  
1840 June 10-11, London (UK)  
1841  
1842 Deendarlianto, Höhne T., Lucas D., Vierow K., 2012, Gas–liquid countercurrent two-phase flow in a PWR hot  
1843 leg: A comprehensive research review, *Nuclear Engineering and Design*, 243, 214– 233

1844 Edwards A.R., O'Brien T.P., 1970, Studies of phenomena connected with the depressurization of water reactors,  
1845 Journal of the British Nuclear Energy Society, 9, 125-135  
1846  
1847 Faucher E., Heradc J-M., Barret M., Toulemonde C., 2000, Computation of Flashing Flows In Variable  
1848 Cross-Section Ducts, Int. J. of Computational Fluid Dynamics,13, 4, 365-391  
1849  
1850 Galetti M.R., D'Auria F., 2004, Technical and regulatory concerns in the use of best estimate methodologies in  
1851 LBLOCA analysis licensing process, International Meeting On Best-Estimate Methods in Nuclear Installation  
1852 Safety Analysis (BE-2004) IX, Washington D.C. (US), Nov. 14-18, ISBN 089448-681-0  
1853  
1854 Glaeser H., Karwat H., 1993, The contribution of UPTF experiments to resolve some scale-up uncertainties in  
1855 countercurrent two phase flow, Nuclear Engineering and Design, 145  
1856  
1857 Gonzales-Gonzales R., Petruzzi A., D'Auria F., Mazzantini O., 2014, Identification of limiting case between DBA  
1858 and SBDBA (CL break area sensitivity): A new model for the boron injection system, Nuclear Engineering and  
1859 Design, 275, 1-10  
1860  
1861 Groeneveld D.C., Leung L.K.H., Kirillov P.L., Bobkov V.P., Smogalev I.P., Vinogradov V.N., Huang X.C., Royer  
1862 E., 1996, The 1995 look-up table for critical heat flux in tubes, Nuclear Engineering and Design, 163, 1-23  
1863  
1864 GRNSPG, 2010, <Atucha-II> FSAR Chapter 15, Section 15.0: Introduction to the Accident Analyses, University  
1865 of Pisa, GRNSPG, RL 700(10), rev. 3, Pisa (I), pp 1-2300, October  
1866  
1867 Hamouda O., Weaver D. S., Riznic J. R., 2018, Transient two-phase blowdown: Experiments and analysis,  
1868 International Journal of Multiphase Flow, 104, 307-321  
1869  
1870 Heckmann K., Sievers J., 2018, Leak-before-break analyses of PWR and BWR piping concerning size effects,  
1871 Nuclear Engineering and Design, 326, 383-391  
1872  
1873 Hewitt G.F., Delhaye J.M., Zuber N. (Eds.), 1992, Post-Dryout Heat Transfer, CRC Press, Boca Raton, FL, USA  
1874  
1875 Hosford S.B., Mattu R., Meyer R.O., Throm E.D., Tinkler C.G., 1981, Asymmetric Blowdown Loads on PWR  
1876 Primary Systems, USNRC NUREG/0609, Washington (DC, US), pp 1-88  
1877  
1878 IAEA, 2000, Safety of Nuclear Power Plants: design, requirements, NS-R-1, Vienna, Austria.  
1879  
1880 IAEA, 2002, [Authors: Allison C., Balabanov E., D'Auria F., Jankowski M., Mišák J. Salvatores S., Snell V.],  
1881 Accident analysis for nuclear power plants, IAEA Safety Reports Series No. 23, ISSN 1020-6450; ISBN  
1882 92-0-115602-2, Vienna, Austria, pp 1-129  
1883  
1884 IAEA, 2007, Use and Development of Coupled Computer Codes for the Analysis of Accidents at Nuclear Power  
1885 Plants, TECDOC 1539 [plus supporting CD], Vienna (A)  
1886  
1887 IAEA, 2008, [Authors: D'Auria F., Glaeser H., Lee S., Mišák J., Modro M., Schultz R.R.], Best Estimate Safety  
1888 Analysis for Nuclear Power Plants: Uncertainty Evaluation, IAEA Safety Report Series, SRS No 52, Vienna (A),  
1889 2008, pp 1-211, ISSN 1020-6450  
1890  
1891 Jo J. C., Jeong J. J., Yun B. J., Moody F. J., 2018, Numerical prediction of a flashing flow of saturated water at high  
1892 pressure, Nuclear Engineering and Technology, 50, 1173-1183  
1893  
1894 Kang D. G., 2016, Analysis of LBLOCA using best estimate plus uncertainties for three-loop nuclear power  
1895 plant power uprate, Annals of Nuclear Energy, 90, 318-330  
1896  
1897 Kastanya D., Boyle S., Hopwood J., Park J. H., 2013, The impact of power coefficient of reactivity on CANDU-6  
1898 reactors, Nuclear Engineering and Technology, 45, 5, 573-580  
1899  
1900 Kendoush A. A., 1989, Measurement of neutron induced nucleation, Nuclear Engineering and Design, 110,  
1901 349-360  
1902

1903 Kim B. J., Kim J., Kim K., Bae S.W., Moon S-K., 2017, Effects of fuel relocation on reflood in a partially-blocked  
1904 rod bundle, Nuclear Engineering and Design, 312, 239–247  
1905  
1906 Kim K.T., 2011, The effect of fuel rod oxidation on PCMI-induced fuel failure, J. of Nuclear Materials, 418, 249–  
1907 260  
1908  
1909 Krieg R., Schlechtendahl E.G., Scholl K.H., 1977, Design of the HDR experimental program on blowdown  
1910 loading and dynamic response of PWR-vessel internals, Nuclear Engineering and Design, 43, 2, 419–435  
1911  
1912 Krieg R., Dolensky B., Granda A., 1982, Core support columns in the upper plenum of a Pressurized Water  
1913 Reactor under blowdown loading II. Three dimensional analysis, calculation of deformation and stresses,  
1914 Nuclear Engineering and Design, 73, 35-44  
1915  
1916 Kurihara R., Ueda S., Miyazono S., 1987, Experimental and analytical studies of pipe whip tests, Nuclear  
1917 Engineering and Design, 103, 253-265  
1918  
1919 Lazarte A. I., Ferreri J. C., 2012, Natural Circulation Characterization of the CNA-II PHWR based on Flow  
1920 Maps using RELAP5. In: 9th International Topical Meeting on Nuclear Thermal-Hydraulics, Operation and  
1921 Safety (NUTHOS-9), N9P0037, Kaohsiung, Taiwan, Sept. 9–13  
1922  
1923 Lee S., Hassan Y.A., Abdulsattar S.S., Vaghetto R., 2014, Experimental study of head loss through an  
1924 LOCA-generated fibrous debris bed deposited on a sump strainer for Generic Safety Issue 191, Progress in  
1925 Nuclear Energy, 74, 166-175  
1926  
1927 Leyse R.H., 2007, letter to Ms. Annette L. Vietti Cook, Secretary USNRC, Rulemaking and Adjudications Staff,  
1928 Public Comment on PRM-50-84: PRM-50-84 and MELLLA+, July 27  
1929  
1930 Lochon H., Daude F., Galon P., Hérard J.M., 2017, Computation of fast depressurization of water using a  
1931 two-fluid model: revisiting Bilicki modelling of mass transfer, Computers and Fluids, 156, pp.162-174.  
1932  
1933 Mahmoodi R., Zolfaghari A., Minuchehr A., 2019, Simulation of pressure waves propagation following LOCA  
1934 in piping systems using Laplace Transform Finite Volume, Annals of Nuclear Energy, 124, 164–171  
1935  
1936 Mascari F., Vella G., Woods B. G., Welter K., D’Auria F., 2012, Analysis of primary/containment coupling  
1937 phenomena characterizing the MASLWR design during a SBLOCA scenario, INTECH Book ‘Nuclear Power  
1938 Plants’, edited by S.H. Chang, ISBN 978-953-51-0408-7, Chapt. 8, pp 203-233  
1939  
1940 Mazzantini O., D’Auria F., Petruzzi A., 2018, Full BEPU application for Chapter 15 of Atucha-2 NPP, ANS Best  
1941 Estimate plus Uncertainty Int. Conf. (BEPU2018), May 13-18, Lucca (I), PL07  
1942  
1943 Moretti F., Terzuoli F., D’Auria F., Mazzantini O., 2018, Instrumentation for full-scale Boron Injection Test  
1944 Facility to support Atucha-2 NPP licensing, Nuclear Engineering and Design, 336, 154-162  
1945  
1946 Muellner N., Petruzzi A., Camargo C., Galetti M. R., D’Auria F., 2008, A proposal for performing Atucha-II  
1947 accident analysis for licensing purposes, A report prepared by DIMNP under the 2<sup>nd</sup> NASA-UniPi Agreement  
1948 to support a formal submittal of NA-SA to ARN, University of Pisa report, 2008-rev.1, July, pp 1-182  
1949  
1950 Nigmatulin B. I., Sopleikov K. I., Blinkov V. N., 1987, Critical steady state blowdown of flashing water through  
1951 tubes, Nuclear Engineering and Design, 99, 85-92  
1952  
1953 Noori-Kalkhoran O., Shirani A. S., Ahangari R., 2016, Simulation of Containment Pressurization in a Large  
1954 Break-Loss of Coolant Accident Using Single-Cell and Multicell Models and CONTAIN Code, Nuclear  
1955 Engineering and Technology, 48, 1140-1153  
1956  
1957 Nouri-Borujerdi A., Ghazani A. S., 2018, A non-equilibrium relaxation model for fast depressurization of  
1958 pipelines, Annals of Nuclear Energy, 111, 1–11  
1959

1960 OECD/NEA/CSNI, 1989, [Lead Authors: Lewis M.J. (Editor), Pochard R., D'Auria F., Karwat H., Wolfert K.,  
1961 Yadigaroglu G., Holmstrom H.L.O.], Thermo-hydraulics of Emergency Core Cooling in Light Water Reactors-A  
1962 State of the Art Report, OECD/CSNI 161, Paris (F), October  
1963  
1964 OECD/NEA/CSNI, 1999, [Authors: Karwat H., Bardelay J., Hashimoto T., Koroll G. W., Krause M., L'Heriteau  
1965 J-P., Lundstrom P., Notafrenesco A., Royl P., Schwinges B., Tezuka H., Tills J., Royen J.], State-of-the-Art Report  
1966 (SOAR) on containment thermalhydraulics and hydrogen distribution, CSNI/R(1999)16, Paris (F)  
1967  
1968 OECD/NEA/CSNI, 2003, Proceedings of the Joint CNRA/CSNI Workshop on "Re-defining the LBLOCA:  
1969 technical bases and its implications" <held in Zurich, June 23-24, 2003>, NEA/CSNI (2003)17 – Vol 1 pp 1-107,  
1970 Vol 2 pp 1-87, Paris (F)  
1971  
1972 OECD/NEA, 2004, [Authors: D'Auria F. (Project Coordinator), Bousbia Salah A., Galassi G.M., Vedovi J.,  
1973 Reventos F., Cuadra A., Gago J.L., Sjoberg A., Yitbarek M., Sandervag O., Garis N., Anherth C., Aragonés J.M.,  
1974 Verdù G., Mirò R., Hadek J., Macek J., Ivanov K., Rizwan-Uddin, Sartori E., Rindelhardt U., Rohde U., Frid V.,  
1975 Panayotov D., Neutronics/Thermal-hydraulics Coupling in LWR Technology – CRISSUE-S WP2:  
1976 State-of-the-Art Report, OECD/NEA Report No 5436, ISBN 92-64-02084-5, Paris (F), Vol. II, pp 1- 293  
1977  
1978 OECD/NEA, 2009, Nuclear Fuel Behavior in Loss-of-coolant Accident (LOCA) Conditions, NEA No. 6846, pp  
1979 1-369, ISBN 978-92-64-99091-3  
1980  
1981 OECD/NEA/CSNI, 2017, [(Lead Authors) Bestion D., D'Auria F. (Ed.), Lien P., Nakamura H., (Contributors)  
1982 Austregesilo H., Skorek T., Bae B.U., Choi K.Y., Kim K.D., Moon S. K., Martinez-Quiroga V., Reventos F.,  
1983 Mascari F., Schollenberger S., Umminger K., Reyes J.N., Rohatgi U.S. Wang W., Zaki T.], Scaling in system  
1984 thermal-Hydraulics applications to Nuclear Reactor safety and design: a State-of-the-Art-Report, NEA/  
1985 CSNI/R(2016)14, JT03411050, Paris, March, pp 1-402  
1986  
1987 Park B. G., Park J. W., Kim C. H., 2011, Experimental study of debris head loss through a pressurized water  
1988 reactor recirculation sump screen after LOCA, Nuclear Engineering and Design, 241, 7, 2462-2469  
1989  
1990 Pecchia M., Parisi C., D'Auria F., Mazzantini O., 2009, Atucha-2 PHWR Monte Carlo MCNP5 and KENO-VI  
1991 Models Development and Application, Int. Conf. on Mathematics, Computational Methods and Reactor  
1992 Physics (M&C), Saratoga Springs, (NY, US), May 3-7  
1993  
1994 Pecchia M., Parisi C., D'Auria F., Mazzantini O., 2015, Application of MCNP for predicting power excursion  
1995 during LOCA in Atucha-2 PHWR, J. Annals of Nuclear Energy, 85, pp 271-278  
1996  
1997 Petruzzi A., D'Auria F., 2005, Relap5/mod3.2 post-test analysis and CIAU uncertainty evaluation of LOFT  
1998 experiment L2-5, Int. Top. Meet. on Nuclear Reactor Thermal-Hydraulics (NURETH-11), Avignon (F), Oct. 2-6  
1999  
2000 Petruzzi A., D'Auria F., 2006, The Internal Assessment of Uncertainty, CIAU and CIAU-TN: Features and key  
2001 Applications, ANS-CNS Top. Meet. On Reactor Physics – PHYSOR, Vancouver (BC, Canada), Sept. 10-14  
2002  
2003 Petruzzi A., Cherubini M., Lanfredini M., D'Auria F., Mazzantini O., 2016, The BEPU Evaluation Model with  
2004 RELAP5-3D for the Licensing of the Atucha-II NPP, Nuclear Technology, 193, pp 113-160  
2005  
2006 Pontillon Y., Ravel S., Parrat D., Ferroud-Plattet M. P., Guérin Y., 2002, Fission gas release under fast transient  
2007 and LOCA conditions: analytical devices implemented at CEA, Tech. Meet <Fuel behavior under transient and  
2008 LOCA conditions>, Halden (Norway), 10–14 Sept. 2001, IAEA TECDOC 1320, Vienna (A)  
2009  
2010 Popov N. K., Snell V. G., 2012, Safety and Licensing Aspects of Power Reactor Reactivity Coefficients, 20<sup>th</sup> Int.  
2011 Conf. on Nuclear Engineering and the ASME 2012 Power Conference, ICONE20-POWER2012-55243, Anaheim,  
2012 (Ca, USA), July 30–Aug.3, 221-230; doi:10.1115/, ISBN: 978-0-7918-4498-4  
2013  
2014 Prosek A., Mavko B., D'Auria F., 2004, Quantitative analysis of RD-14M large LOCA test B9401 calculations, IJS  
2015 Report IJS-DP-8819, Ljubljana (Slo), Jan.  
2016  
2017 Queral C., Montero-Mayorga J., Gonzales-Cadelo J., Jimenez G., 2015, AP-1000 large break LOCA BEPU  
2018 analysis with Trace code, Annals Nuclear Energy, 85, 576-589

2019  
2020 Ranjan R., Banerjee S., Singh R. K., Banerji P., 2014, Local impact effects on concrete target due to missile: An  
2021 empirical and numerical approach, *Annals of Nuclear Energy*, 68, 262–275  
2022  
2023 Ransom V.H., Wang W., Ishii M., 1998, Use of an ideal scaled model for scaling evaluation, *J. Nuclear*  
2024 *Engineering and Design*, 186  
2025  
2026 Raynaud P. A. C., 2012, Fuel Fragmentation, Relocation, and Dispersal during the Loss-of-Coolant Accident,  
2027 USNRC NUREG 2121, March, Washington (D.C., US), pp 1-127  
2028  
2029 Reid S.R., Wang B., Aleyaasin M., 2011, Structural modelling and testing of failed high energy pipe runs: 2D and  
2030 3D pipe whip, *Int. J. of Pressure Vessels and Piping*, 88, 189-197  
2031  
2032 RELAP5/MOD3, 1998, Code manual volume I: code structure, system models and solution procedure,  
2033 NUREG/CR-5535, USNRC, Washington, DC, USA  
2034  
2035 Reventos F., Perez M., Batet L., Pericas R. (Coordinators), Toth I., Bazin P., De Crecy A., Borisov S., Glaeser H.,  
2036 Skorek T., Joucla J., Probst P., Ui A., Chung B., Oh D., Kyncl M., Pernica R., Manera A., D’Auria F., Petruzzi A.,  
2037 Del Nevo A., 2008, Simulation of a LBLOCA in Zion Nuclear Power Plant - BEMUSE Phase IV Report,  
2038 OECD/NEA/CSNI/ R(2008)6 vol 1, JT03256246, Paris (F)  
2039  
2040 Rohatgi U.S., Glaeser H., 2019, Counter Current Flow Limitation (CCFL), this Special Issue [MDPI. Fluids]  
2041  
2042 Rozzia D., Del Nevo A., Adorni M., D’Auria F., 2012, Modeling of BWR Inter-Ramp Project experiments by  
2043 means of TRANSURANUS code, *Annals of Nuclear Energy*, 50, 238–250  
2044  
2045 Sartoris C., Taisne A., Petit M., Barré F., Marchand O., 2010, A consistent approach to assess safety criteria for  
2046 reactivity initiated accidents, *Nuclear Engineering and Design*, 240, 57-70  
2047  
2048 Shiozawa S., Saito S., Yanagihara S., 1982, Zircaloy-UO2 and -Water Reactions and Cladding Temperature  
2049 Estimation for Rapidly-Heated Fuel Rods under an RIA Condition, *J. of Nuclear Science and Technology*, 19, 5,  
2050 368-383  
2051  
2052 Svanholm K., Breggi M.P., D’Auria F., Ianiri R., 1995, Halden Reactors IFA-511.2 and IFA-54X: Experimental  
2053 Series under Adverse Core Cooling Conditions, *Experimental Thermal and Fluid Science*, 11, 77-100  
2054  
2055 Thadani A, Laaksonen J., 2003, Workshop Summary “Re-defining the LBLOCA: technical bases and its  
2056 implications”, June 23-24, Zurich (CH), NEA/CSNI(2003)17, Paris (F), Vol I, pp 15-17  
2057  
2058 Ullah Amin S. A., Bang Y. S., Lee J. S., 2017, Assessment of post-LOCA long term cooling considering the  
2059 in-vessel downstream effect, *Annals of Nuclear Energy*, 110, 63–72  
2060  
2061 Urbanic V.F., Heidrick T. R., 1978, High-temperature oxidation of zircaloy-2 and zircaloy-4 in steam, *J. of*  
2062 *Nuclear Materials*, 75, 2, 251–261  
2063  
2064 USAEC, 1971, Interim Acceptance Criteria (IAC) for ECCS, USAEC, Washington, DC, USA  
2065  
2066 USNRC, 1978, Standard Format and Content of Safety Analysis Report for Nuclear Power Plants—LWR  
2067 Edition, USNRC Regulatory Guide 1.70, Washington, DC, USA  
2068  
2069 USNRC, 2005, Transient and accident analysis methods, RG 1.203, USNRC, Washington, DC, USA  
2070  
2071 USNRC, 2007, NUREG-0800: Standard Review Plan Section 4.2: Fuel System Design, Appendix B—Interim  
2072 Acceptance Criteria and Guidance for the Reactivity Initiated Accidents, USNRC, NUREG 0800, Washington  
2073 DC, USA  
2074  
2075 USNRC, 2013, Standard Review Plan for the Review of Safety Analysis Reports for Nuclear Power Plants  
2076 (continuously updated), NUREG 0800, Washington, DC, USA  
2077

2078 USNRC, 2018, Regulatory Guide 1.224, Preliminary Draft (Draft was issued as DG-1263, dated March 2014),  
2079 Establishing Analytical Limits for Zirconium-Alloy Cladding Material, Washington (D.C., US), pp 1-32  
2080  
2081 Valette M., Pouvreau J., Bestion D., Emonot P., 2011, Revisiting large break LOCA with the CATHARE-3  
2082 three-field model, Nuclear Engineering and Design, 241, 4487-4496  
2083  
2084 Vigni P., D'Auria F., Rosa U., 1978, Blowdown experiments from a pressure vessel with internal structures, (in  
2085 Italian), University of Pisa Report, IIN - RL 317(78), Pisa (I), Dec. 1978, pp 1-65  
2086  
2087 Vigni P., D'Auria F., 1979, Unsteady Two-Phase Jet Forces (in Italian), J. Ingegneria Nucleare, 10, 23-32  
2088  
2089 Wolf L., 1982, Experimental results of coupled fluid-structure interactions during blowdown of the HDR-vessel  
2090 and comparisons with pre-and post-test predictions, Nuclear Engineering and Design, 70, 3, 269-308  
2091  
2092 Yano T., Miyazaki N., Isozaki T., 1982, Transient analysis of blowdown thrust force under PWR LOCA, Nuclear  
2093 Engineering and Design, 75, 157-168  
2094  
2095 Ylonen A., 2008, Large break blowdown test facility study, Master thesis at University of Lappeenranta,  
2096 Lappeenranta (Finland)  
2097  
2098 Zhang T., Brust F. W., Wilkowski G., Xu H., Betervide A. A., Mazzantini O., 2013, Leak-Before-Break Under  
2099 Beyond Design Basis Seismic Loading, ASME J. of Pressure Vessel Technology, 135, 1-9  
2100